

Aus der Intensive Care Unit, Universitätskliniken Basel
Arbeit unter der Anleitung von PD Dr. Patrick Hunziker und Dr. Emmanuel
Delamarche

**Nanotechnology in Medicine:
First Application of Micromosaic Immunoassays to Human Samples**

Inauguraldissertation
zur Erlangung der Doktorwürde der gesamten Heilkunde
vorgelegt der Medizinischen Fakultät der Universität Basel

von

Marc Philippe Wolf, Bern

Von der Medizinischen Fakultät der Universität Basel genehmigt auf Antrag

von Prof. Dr.

Koreferent

Tag der Promotion:

Table of Contents

ACKNOWLEDGEMENTS v ABBREVIATIONS v

1 ABSTRACT / ZUSAMMENFASSUNG 1

2 INTRODUCTION 3

- 2.1 Point-of-Care Testing 3
- 2.2 Miniaturization of Bioassays 4
- 2.3 Microfluidic Networks 4
- 2.4 Adsorption of Proteins from a Liquid to a Solid Phase 7
- 2.5 Non-Competitive, Solid Phase, ‘Sandwich’, Fluorescence Immuno-assay 8
- 2.6 C-reactive Protein 9
- 2.7 Pathophysiology of Acute Myocardial Infarctions 11
- 2.8 Contact Angle Goniometry 11
- 2.9 X-Ray Photoelectron Spectroscopy 12
- 2.10 Ellipsometry 13
- 2.11 Affinity Chromatography 14
- 2.12 Polydimethylsiloxane 14
- 2.13 Self-Assembled Monolayers of Thiols on Gold 15

3 EXPERIMENTAL SECTION 18

- 3.1 Solid Phase Substrate 18
- 3.2 Fabrication of Microfluidic Networks 18
- 3.3 Surface Preparation of the Silicon Wafer 18
- 3.4 Surface Characterization of the Silicon Wafer 19
- 3.5 Chemicals and Biochemicals 20
- 3.6 Image Acquisition 20

4 RESULTS 22

- 4.1 Patterned Delivery of Proteins with Microfluidic Networks 22
- 4.2 Working Procedure of a Micromosaic Immunoassay 24
- 4.3 Optimization of the Wafer Surface 25

4.4	Does Significant Depletion of Capture Antibody Occur inside Channels? 31
4.5	Does Variation of pH Significantly Change Binding Rates? 32
4.6	Capture and Detection Antibody Concentrations 32
4.7	Time Dependency of Analyte Binding 34
4.8	Assay Variance and Spot Quality 36
4.9	Reference Curve 37
4.10	Detecting Multiple Markers in Human Plasma Simultaneously 38

5 DISCUSSION 40

6 CONCLUSION 43

APPENDIX A – PUBLICATIONS 44

ACKNOWLEDGEMENTS

University Hospital Basel – Department of Research

Patrick Hunziker, Christian Zaugg, Beat Erne, Vreni Spoerri, Frances Kern.

University of Basel – Department of Physics – Condensed Matter Group

Christian Schoenenberger, François Dewarrat.

University of Basel – Biocenter Basel

Jeannette Wolf, Duc Luu.

IBM Zurich Research Laboratories – Rueschlikon

Bruno Michel, David Juncker, Emmanuel Delamarche, Heiko Wolf, Alex Bietsch, Matthias Geissler, Sergey Amontov, Ute Drechsler, Michel Despont, Richard Stutz.

ABBREVIATIONS

μ FN	microfluidic network	PDMS	polydimethylsiloxane
μ MIA	micromosaic immunoassay	PEG	polyethyleneglycol
Ab	antibody	POC	point-of-care
AMI	acute myocardial infarction	S100	protein S-100
BNP	brain natriuretic peptide	SAM	self-assembled monolayer
BSA	bovine serum albumin	SI	systemic inflammation
CHD	coronary heart disease	SPI	solid phase immunoassay
CRP	C-reactive protein	TnI	troponin-I
cTnI	cardiac Troponin-I	α BNP	anti-BNP antibody
cTnT	cardiac Troponin-T	α CRP	anti-CRP antibody
ECT	eicosanethiol	α Mb	anti-myoglobin antibody
FITC	fluoresceine-isothiocyanate	α S100	anti-S100 antibody
Mb	myoglobin	α TnI	anti-TnI antibody
PBS	phosphate buffered saline		

1 ABSTRACT / ZUSAMMENFASSUNG

Background: Point-of-care (POC) testing is the idea to measure rapidly biomarkers near patients. Nanotechnology offers a spectrum of new techniques that promise to revolutionize medicine. So-called passive microfluidic networks i.e. miniaturized channels that guide minute amounts of liquids across a surface are especially promising for a new generation of immunoassays, as they allow testing of a large number of analytes in a minimum of time with a minimum amount of reagents. The applicability of such devices to clinically important disease markers in human plasma samples has not yet been investigated.

Aim: To investigate the feasibility, sensitivity, reproducibility of the micromosaic immunoassay (μ MIA) to detect biomarkers in spiked human plasma samples.

Method: We use passive microfluidic networks with 8 channels on a Si wafer to perform simultaneously up to 64 miniaturized solid phase immunoassays in a combinatorial fashion (i.e. one μ MIA). These assays are distributed on a $180 \times 180 \mu\text{m}^2$ area and are analyzed by fluorescence microscopy.

Results: We optimized the surface chemistry of the wafer, the capture and detection antibody concentrations, and the analyte incubation time. A μ MIA can be performed within ~8 min. The sample volume required for multiple analyte detection is only ~2 μL . The detection limit for the cardiac marker C - reactive protein in human plasma is $0.03 \mu\text{g mL}^{-1}$. The intra-assay variance is 4.4%. The quality of the assay pattern was analyzed. We also detected simultaneously five different cardiac markers in human plasma with one μ MIA.

Conclusions: This is the first experimental demonstration of the feasibility to detect proteins in human plasma with μ MIAs. The reported sensitivity, reaction time, and intra-assay variance are better or equal to clinical laboratory testing. The results demonstrate the feasibility of μ MIAs to measure biomarkers in human plasma samples and indicate the potential of μ MIAs for laboratory and POC testing.

Hintergrund: Point-of-care (POC) Testen ist der Ansatz, Biomarker in kurzer Zeit patientennah zu messen. Die Nanotechnologie bietet ein Spektrum neuer Techniken die versprechen, die Medizin zu revolutionieren. Sogenannt passive Microfluidic Networks, d.h. miniaturisierte Kanäle die kleinste Flüssigkeitsmengen über ein Oberfläche leiten, sind vielversprechend für eine neue Generation von Immunoassays, da sie Messungen einer Vielzahl von Proben in kurzer Zeit und mit einem Minimum an Reagentien ermöglichen. Die Anwendbarkeit dieser Technik für klinisch relevante Krankheitsmarker in menschlichem Plasmaproben wurde bisher noch nicht untersucht.

Ziel: Die Zweckmässigkeit, Sensitivität, Reproduzierbarkeit des Micromosaic Immunoassays (μ MIA) zur Messung von Biomarkern in gespiktem menschlichem Plasmaproben untersuchen.

Methode: Wir verwenden passive ‚microfluidic networks‘ mit 8 Kanälen auf einem Si Wafer zum gleichzeitigen Durchführen von bis zu 64 miniaturisierten heterogenen Immunoassays auf eine kombinatorische Art (d.h. ein μ MIA). Diese Assays sind verteilt auf einer Fläche von $180 \times 180 \mu\text{m}^2$ und werden per Fluoreszenzmikroskopie analysiert.

Resultate: Wir optimierten die Oberflächenchemie der Wafer, die Konzentrationen von ‚capture‘ und ‚detection‘ Antikörpern und die Inkubationszeit des Analyten. Ein μ MIA kann innerhalb von ~8 min durchgeführt werden. Das notwendige Probevolumen beträgt nur ~2 μ L. Die Detektionsgrenze des Herzmarkers C-reaktives Protein in menschlichem Plasma beträgt $0.03 \text{ } \mu\text{g mL}^{-1}$. Die Varianz innerhalb eines μ MIA beträgt 4.4%. Die Qualität des Depositionsmusters der Assays wurde untersucht. Wir bestimmten auch 5 verschiedene Herzmarker gleichzeitig mit einem μ MIA.

Schlussfolgerungen: Die gemessene Sensitivität, Reaktionszeit und Varianz innerhalb eines μ MIA sind vergleichbar mit herkömmlichen Labormethoden und bestätigen ein Potential der μ MIA in einem portablen Testsystem verwendet zu werden.

2 INTRODUCTION

2.1 Point-of-Care Testing

In recent time, a major interest of the fabrication of diagnostic instruments has been the miniaturization towards portability, simplicity of handling, reduction of time lapse from sample introduction to test result and the implementation of multiple clinical parameter determinations.¹ This allows the displacement of measurements from a central laboratory directly to the bedside, which is called point-of-care (POC) testing or near-patient testing.² The reason for this development is the urge to make rapid decisions in emergency triage of patients presenting with unspecific, but potentially life-threatening, symptoms. In emergencies, the transport of blood samples from the location of treatment to a laboratory can substantially increase the time to treatment. Besides diagnostics, the surveillance of stationary patients, especially of the critical care units, could also benefit from near-patient testing. Measuring crucial parameters in short intervals could contribute to a fast therapeutic intervention upon pathophysiologic events and a more accurate and specific treatment of disease states. Specifically designed test kits would allow the rapid availability of critical parameters.³ Difficulties with the integration and quality management of near patient testing outside laboratories with conventional standards have been stated.⁴ POC testing is performed in outpatient centres has also been mentioned as a survival strategy for American clinical laboratories, which are rivalled by more cost effective managed care organizations (MCOs).⁵

A test kit specifically designed for the detection or exclusion of AMI could contain sensing areas for the following serum markers: C-reactive protein (CRP), myoglobin, cardiac Troponin-I (cTnI) or cardiac Troponin-T (cTnT) and D-Dimer.

Point-of-care kits for Troponin already exist; they are mainly used in emergency stations. Many of them use a membrane-based immunoreaction, resulting in the visibility of a stripe of nano-gold particle derivatized antibodies indicating a positive result.⁶ It is the same principle used in pregnancy stripe tests that measure the beta-HCG content of urine. These tests are qualitative, only some are more elaborate and present semiquantitative results (usually tertile or quartiles of concentration). Generally, quantitative results are more desirable because they allow more accurate decision taking.

¹ Bingham D, Kendall J, Clancy M. The portable laboratory: an evaluation of the accuracy and reproducibility of i-STAT. Ann Clin Biochem. 1999; 36, 66.

² Hudson MP, Christenson RH, Newby LK, Kaplan AL, Ohman EM. Cardiac markers: point of care testing. Clin Chim Acta. 1999; 284, 223.

³ Maisel AS, Koon J, Krishnaswamy P, Kazenegra R, Clopton P, Gardetto N, Morrisey R, Garcia A, Chiu A, De Maria A. Utility of B-natriuretic peptide as a rapid, point-of-care test for screening patients undergoing echocardiography to determine left ventricular dysfunction. Am Heart J. 2001; 141, 367.

⁴ Plebani M , Zaninotto M. Cardiac markers: centralized or decentralized testing? Clin Chem Lab Med. 1999; 37(11/12), 1113.

⁵ Takemura Y, Beck JR. Laboratory testing under managed care dominance in the USA. J Clin Path. 2001; 54, 89.

⁶ Mueller-Bardorff M, Rauscher T, Kampmann M, Schoolmann S, Laufenberg F, Mangold D, Zerback R, Remppis A, Katus HA. Quantitative bedside assay for cardiac Troponin T: a complementary method to centralized laboratory testing. Clin Chem. 1999; 7, 1002.

2.2 Miniaturization of Bioassays

Miniaturization of assays for determination of biological parameters in patient samples appears to be appealing because of reduced cost per result. Rapid analysis achieved in this way would also allow rapid therapeutic intervention.⁷ However, the availability of an abundant amount of results is not always desirable, as the specificity of the tests will never reach hundred percent, and therefore false positive results will always be included, which will have to be further investigated, providing a source of unnecessary consumption of infrastructure and budget. Nevertheless, we are convinced of the advance of miniaturized test systems in the clinic. An effort to tailor the testing systems to clinical requirements has to be outperformed carefully in order to fully profit of facilitated data gain. Besides the health care sector, the pharmaceutical industry has a major interest in the availability of microscale assays for massively parallel drug discovery.⁸ Applications for toxicology are also being developed.⁹ An overview of current microarray technology and applications can be found in Kricka, 2001.¹⁰

2.3 Microfluidic Networks

In solid phase immunoassays (SPI), the limiting factor seems to be mass transport, which is driven by Brownian movement (diffusion). Efforts therefore tend towards miniaturization of wells in classical SPI, where one wants to reduce diffusion distance and thus minimize time required for saturation of surface. One problem encountered there is the increase of the quotient surface by volume, which can trouble saturation.¹¹ Also commonly used are shakers in order to move the fluid in the wells to speed up mass transport by convection. The advantage of particle-based assays is their short reaction time for specific binding of analyte. The particles are entirely immersed in the fluid and they abide Brownian movement, they can therefore bind much more target molecules over time than a surface-immobilized antibody. Furthermore, there is no formation of a gradient towards the antibodies, as happens in standard SPI, where the analyte starts to become depleted in the intimate vicinity of the surface, thus contributing to the formation of large diffusion distances. Thus, incubation time for specific binding and blocking of the surface in standard SPI requires normally up to some hours. We describe the importance of the availability of rapid results in the clinic in the following section. Particle based immunoassays function most commonly with antibodies (or antigens) immobilized on latex particles. The change in turbidimetry and nephelometry can be measured by illumination with a laser and capture of the deviated light fraction by photo diodes. By means of the constant flow inside the channels and the micrometer range size, microfluidic networks provide both, small diffusion distances from bulk

⁷ Kricka LJ. Miniaturization of analytical systems. Clin Chem. 1998; 9, 2008.

⁸ Rademann J, Jung G. Integrating combinatorial synthesis and bioassays. Science. 2000; 287, 1947.

⁹ Rowe-Taitt CA, Golden JP, Feldstein MJ, Cras JJ, Hoffman KE, Ligler FS. Array biosensor for detection of biohazards. Biosensors and bioelectronics. 2000; 14, 785.

¹⁰ Kricka LJ, Fortina P. Microarray technology and applications: an all language literature survey including books and patents. Clin Chem. 2001; 8, 1479.

¹¹ Silzel JW, Cercek B, Dodson C, Tsay T, Obremski RJ. Mass-sensing, multianalyte microarray immunoassay with imaging detection. Clin Chem. 1998; 9, 2036.

to surface and sufficient supply of molecules. They seem to be the ideal tool for rapid analysis (a few minutes), requiring only tiny amounts of solution (less than 500 nL). In Figure 1 the principle of the driving force of the flow in the channels, the contact angles of water with the surface, is demonstrated. Low contact angles correlate with fast filling. Laminar flow of a liquid in a capillary follows the equation

$$v = \frac{C_g \Delta p}{\eta l} \quad (1)$$

The mean speed v of a liquid is proportional to the pressure drop, Δp , driving a volume of liquid filling the channel over a length l . The factor C_g / η is a friction parameter, or dissipation term. C_g contains the geometric boundaries of the capillary and η is the viscosity. The pressure drop is described by

$$P_c = \gamma \left\{ \frac{\cos \theta_{PDMS} + \cos \theta_{PEG}}{a} + \frac{2 \cos \theta_{PEG}}{b} \right\} \quad (2)$$

where b is the width and a the height of the channels, γ the surface tension of the liquid and θ_{PEG} and θ_{PDMS} the contact angles of the liquid on PEG and PDMS respectively. The average contact angle of for thiol-PEGs is 40 deg whereas on thiol-ECT it is 110 deg. Ideal would be a contact angle of 0 deg inside the channels and of 180 deg outside the channels. Figure 2 shows the relation between depletion of proteins in the channels after 10 seconds and the size of the channels. The concentration gradient in small channels is larger for the distance from surface to the fast flowing region in the middle of the channel, which means, that rapid diffusion is sustained by rapid supply of molecules. In Figure 3, the velocity profile inside channels is shown in dependency of the distance passed from the entry port.

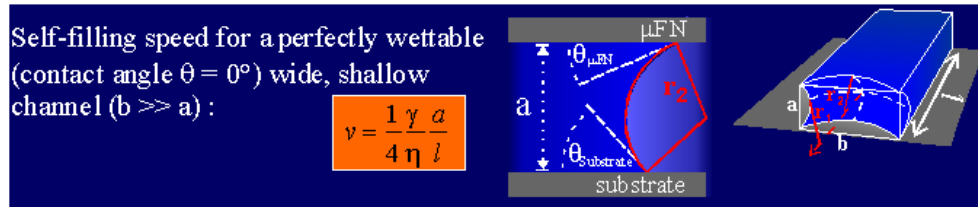


Figure 1. Self-filling speed in perfectly wettable channel with a scheme of the contact angles in the channel. [fig. by D. Juncker]

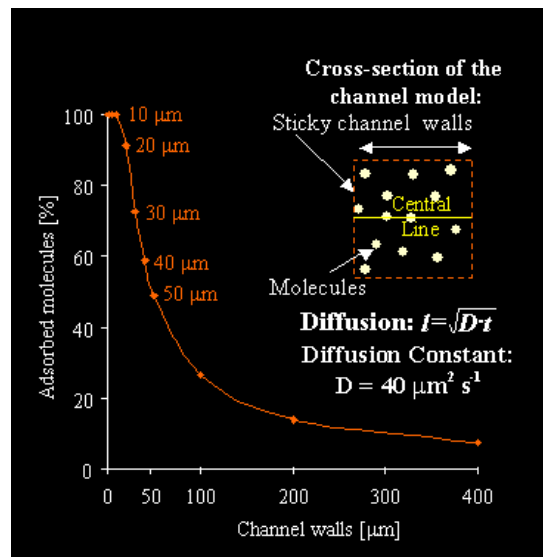


Figure 2. Fraction of the adsorbed molecules after an incubation time of 10 s as a function of the distance of capillary walls. [fig. by D. Juncker]

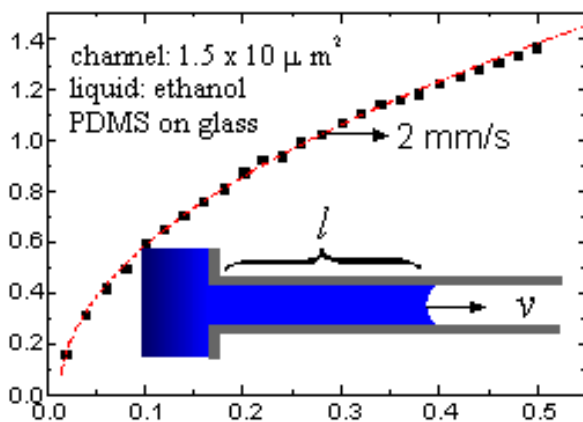


Figure 3. The X-axis represents the time in seconds, the y-axis the length l in mm. The filling speed decreases with increasing distance from the filling port, because resistance increases proportionally with length of the filled channel section. [Fig. by D. Juncker]

Physisorption of proteins to a surface (non-specific binding) is a fast process. Its speed can be calculated by measuring the gradient of adsorbed proteins in protein-depleted channels (Figure 4).



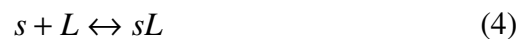
Figure 4. Low concentrations of proteins in solutions tend to deplete by surface adsorption with increasing distance from the filling port. The length of the depletion gradients can be used to calculate the adsorption time of proteins. [fig. from ref. 69]

Physisorption takes place in some milliseconds and therefore is not a limiting factor in process speed. In contrast to NSA, specific binding of proteins

requires their proper orientation in order to expose their epitope to the variable region of the antibody or inversely. Estimations of the time required for proper formation of this bond and the time required for sufficient saturation (more than 95%) cannot be assessed by performing classical SPI, as their limiting factor is the mass transport of molecules. A time series to estimate the influence of binding kinetics on signal strength has been done. Its outcome is presented in the results section.

2.4 Adsorption of Proteins from a Liquid to a Solid Phase

The Scatchard model is the most widely used mathematical approach to the quantitative description of the multiple equilibria taking place when a binder (e.g. an antibody) binds reversibly to a ligand molecule, L (antigen, analyte).



The Scatchard Model focuses on the individual binding sites of the binder and applies the law of mass action for each site, s, defining the association constant (affinity constant) K and assuming that the affinity of each particular site for the ligand is not influenced by the extent of occupancy of the other sites (independent and non-interacting binding sites). Thus,

$$K = \frac{B}{F(N - B)} \quad (5)$$

where B and F represent the concentrations (molarities) of the bound and free (unbound) ligand respectively, and N is the total concentration of the binding sites. N is given by the product of the total binder concentration times the number of binding sites per binder molecule. N – B represents the concentration of unoccupied (free) binding sites on the binder molecule. However, protein functionality changes with adsorption on solid phases.¹² Upon adsorption, physical rearrangements in the conformation of proteins occur, depending both, on properties of the surface¹³ and of the protein density on the surface¹⁴ and of the electrolyte environment of the solution, due to co-adsorption of electrolyte molecules.¹⁵ Steric hindrance and molecule orientation can trouble the proper exposure of bound molecule binding sites to the liquid phase. Furthermore, relative size of the analyte and the tracer (label) and the method of immobilization of the antibody influence the performance

¹² Butler JE, Ni L, Nessler R, Joshi KS, Suter M, Rosenberg B, Chang J, Brown WR, Cantarero LA. The physical and functional behaviour of capture antibodies adsorbed to polystyrene. *J Imm Meth*. 1992; 150, 77.

¹³ Elgersma AV, Zsom RLJ, Lyklema J, Norde W. Adsorption competition between albumin and monoclonal immuno-gamma-globulins on polystyrene lattices. *J Colloid and Interface Science*. 1992; 152, 410.

¹⁴ Wimalasena RL, Wilson GS. Factors affecting the specific activity of immobilized antibodies and their biologically active fragments. *J Chromatography, Biomedical Applications*. 1991; 572, 85.

¹⁵ Lyklema J. Proteins at solid-liquid interfaces, a colloid-chemical review. *Colloids and Surfaces*. 1984; 10, 33.

of immunoassays.¹⁶ Dynamic measurements reveal the non-uniformity of Langmuir curves with experimental data.¹⁷ Thus, these experimental data clearly indicate the limitations of the Scatchard model. Nevertheless, it is very useful for the approximate statistical evaluation of immunoassay dynamic range (performance).

2.5 Non-Competitive, Solid Phase, ‘Sandwich’, Fluorescence Immunoassay

The immunoassay binding makes profit of the specific binding of the variable region of antibodies (immunoglobulin G or IgG) to select regions (epitope) on a target molecule (antigen, analyte). Each antibody possesses two identical binding sites and therefore can potentially bind two antigens simultaneously.

Antibody solutions can either be monoclonal or polyclonal. Antibodies are produced by plasma cells. Each plasma cell only produces antibodies with exactly the same binding specificity. To obtain solutions containing only antibodies of the same specificity, a single plasma cell is fused with spleen myeloma cells in order to enforce proliferation. Clone deriving of this cell will all produce structurally identical antibodies. Solutions of these are termed monoclonal. In contrast, polyclonal solutions derive from multiple plasma cells, as encountered in serum on physiological immune reaction. To isolate the fraction of analyte binding antibodies, affinity chromatography can be performed. The resulting solution will contain antibodies with identical binding specificity but differing binding constants. Monoclonal antibody solutions are therefore better suited for accurate quantitative measurements because they are well defined. An outline of the structure and functionality of antibodies and the immune system can be found in Janeway, 2000.¹⁸

The binding of specific antibodies by the analyte can be made detectable among other by labelling the antibodies with a signal molecule whose concentration can be quantified by radiometry, fluorescence, reflectance or luminescence (corresponding to radioisotope, fluorophore, metal particles, enzymes as labels). In Figure 5, the principle of the sandwich immunoassay is demonstrated. A capture antibody is immobilized on a solid phase (surface). The remaining free area of the surface is blocked by adsorption of BSA or casein to prevent non-specific adsorption of analyte or detection antibody. The surface is then incubated with analyte solution. The capture antibody binds the analyte. The surface is rinsed and detection antibody solution is added. Detection antibodies will bind to the bound analyte, and consecutively allowing the determination of their surface density which is proportional to the amount of analyte in the analyte solution (given that saturation of capture antibodies with analyte has not been reached).

¹⁶ Schramm W, Paek SH. Antibody-antigen complex formation with immobilized immunoglobulins. *An Biochem*. 1992; 205, 47.

¹⁷ Bernard A, Bosshard HR. Real-time monitoring of antigen-antibody recognition on a metal oxide surface by an optical grating coupler sensor. *Eur J Biochem*. 1995; 230, 416.

¹⁸ Janeway C, Travers (Eds.). *Immunobiology*, Current Biology Ltd., London, 2000.

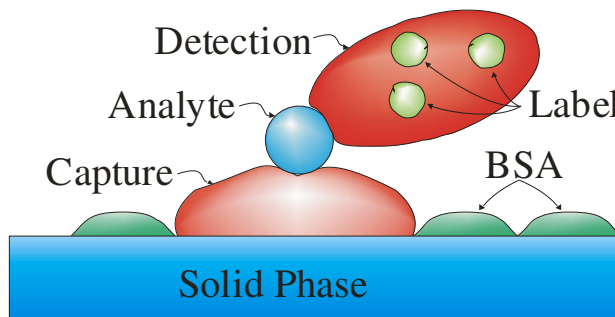


Figure 5. Principle of the sandwich immunoassay. The solid black spots on the detection antibody symbolize label molecules (BSA: bovine serum albumin).

An outline of the development of ligand assays can be read in Ekins, 1998.¹⁹ Further reading on immunoassays can be found in Diamandis, 1996.²⁰

2.6 C-reactive Protein

C-reactive protein (CRP) consists of five identical non-glycosylated subunits and has a molecular weight of 23.0 kD. It is part of the pentraxine protein group, found in all vertebrates and most non-vertebrates. CRP is synthesized in the liver upon stimulation with IL-6 (interleukin 6), a signal substance of the leucocytes.²¹ Its concentration in adults and children is $0.068 - 8.2 \text{ mg L}^{-1}$, with a median of 0.58 mg L^{-1} .^{22,23} (higher values are reported in a recent study),²⁴ where age and female sex contribute to slightly raised values.²⁵ The serum level of CRP increases within 6 hours after a trauma and reaches its peak after 48 hours.²⁶ An inflammation produces raised levels of CRP (although not necessary, as e.g. for Colitis ulcerosa).²⁷ The clinical threshold has been set to 10 mg L^{-1} , values greater than 100 mg L^{-1} can be observed in systemic bacterial inflammations, where sepsis with gram-negative bacteria produces levels up to 500 mg L^{-1} . Its main role remains uncertain. As no genetic variation of its gene has been observed, it is most probably essential for vertebrate life. Some functions include binding to endogenous and exogenous ligands in the presence of calcium, e.g. particle of necrotic cells, to

¹⁹ Ekins RP. Ligand assays: from electrophoresis to miniaturized microarrays. Clin Chem. 1998; 9, 2015.

²⁰ Diamandis EP, Christopoulos TK (Eds.) Immunoassay. Associated Press, New York, 1996.

²¹ Weinhold B, Ruther U. Interleukin-6-dependent and -independent regulation of the human C-reactive protein gene. Biochem J. 1997; 327, 425.

²² Marhaug G, Dowton SB. Serum amyloid A: apolipoprotein and precursor of AA amyloid. In: Husby G, ed. Reactive Amyloidosis and the Acute Phase Response. Ballieres Clinical Rheumatology, Vol 8, no. 3, Balliere Tindall, London, 1994; 533.

²³ Kindmark CO. The concentration of C-reactive protein in sera from healthy individuals. Scand J Clin Lab Invest. 1972; 29, 407.

²⁴ Price CP, Calvin J, Walker SA, Trull A, Newman DJ, Gorman EG. A rapid and sensitive automated light scattering immunoassay for serum C-reactive protein and the definition of a reference range in healthy blood donors. Clin Chem Lab Med. 1999; 37(2), 109.

²⁵ Hutchinson WL, Koenig W, Froehlich M, Sund M, Lowe GDO, Pepys MG. Immunoradiometric assay of circulating C-reactive protein: age-related values in the adult general population. Clin Chem. 2000; 7, 934.

²⁶ Colley CM, fleck A, Goode AW, Muller BR, Myers MA. Early time course of the acute phase response in man. J Clin Pathol. 1983; 36, 203.

²⁷ Tillet WS, Francis T. Serological reactions in pneumonia with a non-protein somatic fraction of pneumonococcus. J Exp Med 1930; 52, 561.

cell membranes with defect lipid bilayer presenting internal phospholipids, phosphorylcholin from cell membranes of bacteria, fungus and parasites. It can contribute to their elimination by opsonisation. Bound to a ligand it can activate the complement system over the classical pathway, bind directly to receptors (FcXR1) on phagocytes and lymphocytes (IgG-FcR), and precipitate ligands.²⁸ The time course of CRP serum levels after myocardial infarction has been proposed as an independent prognostic marker after AMI.^{29,30} In recent times, the correlation between atherosclerotic plaques and elevated levels of CRP has been investigated on its usability as a prognostic marker in future atherosclerotic lesions, especially in the coronary arteries.³¹ It has been observed, that raised levels of CRP correlate with an increased risk of succumbing AMI by vessel occlusion. Association of pre-treatment CRP levels with unstable angina and specific high risk features of coronary lesions determined with coronary angiography has been shown.^{32,33} CRP as a strong, independent predictor of future coronary events, comparable to the prognostic significance of serum LDL values, has been proposed.³⁴ Consistency of these findings has been demonstrated in meta-analysis of prospective studies.^{35,36} Intraindividual diurnal variation of CRP levels in healthy subjects has been shown to be neglectable when quintiles of CRP levels are used for clinical assessment, whereas IL-6 shows significant variations.³⁷ Some authors point out the questions arising from the significant fall of CRP levels upon initiation of treatment with statins (HMG-CoA reductase inhibitors) significantly before their action on the serum lipid metabolism on the possible mechanism of their

²⁸ Agrwal A, Kilpatrick JM, Voanakis JE. Structure and function of human C-reactive protein. In: Mackiewicz A, Kyshner I, Baumann H, eds. Acute phase proteins. London: CRC Press, 1993, p79.

²⁹ De Winter RJ, Fischer JC, de Jongh T, van Straalen JP, Bholasingh R, Sanders GTB. Different time frames for the occurrence of elevated levels of cardiac Troponin T and C-reactive protein in patients with acute myocardial infarction. Clin Chem Lab Med. 2000; 38(11), 1151.

³⁰ Roberts WL, Sedrick R, Moulton L, Spencer A, Rifai N. Evaluation of four automated high-sensitivity C-reactive protein methods: implications for clinical and epidemiological applications. Clin Chem. 2000; 4, 461.

³¹ Van Lente F. Markers of inflammation as predictors in cardiovascular disease. Clin Chim Acta. 2000; 293, 31.

³² Koenig W, Sund M, Froehlich M, Fischer HG, Loewel H, Doering A, Hutchinson WL, Pepys MB. C-reactive protein, a sensitive marker of inflammation, predicts future risk of coronary heart disease in initially healthy middle-aged men. Circulation. 1999; 99, 237.

³³ Katsiris D, Korovesis S, Giazitzoglou E, Parissis J, Kalivas P, Webb-Peploe MM, Ioannidis JPA, Haliassos A. C-reactive protein concentrations and angiographic characteristics of coronary lesions. Clin Chem. 2001; 5, 882.

³⁴ Rifai N, Ridker PM. High-sensitivity C-reactive protein: a novel and promising marker of coronary heart disease. Clin Chem. 2001; 3, 403.

³⁵ Danesh J, Collins R, Appleby P, Peto R. Association of fibrinogen, C-reactive protein, albumin, or leukocyte count with coronary heart disease. JAMA. 1998; 279, 1477.

³⁶ Danesh J, Whincup P, Walker M, Lennon L, Thomson A, Appleby P, Gallimore RJ, Pepys MB. Low grade inflammation and coronary heart disease: prospective study and updated meta-analyses. BMJ. 2000; 321, 199.

³⁷ Meier-Ewert HK, Ridker PM, Rifai N, Price N, Dinges DF, Mullington JM. Absence of diurnal variation of C-reactive protein concentrations in healthy human subjects. Clin Chem. 2001; 3, 426.

action.³⁸ Standardization of high sensitivity automated assays is a topic of concern,³⁹ as in general is the immunoassay standardization.⁴⁰

2.7 Pathophysiology of Acute Myocardial Infarctions

When a blood vessel is obstructed (this commonly happens in acute myocardial infarction (AMI) by embolism, when a thrombus, usually from the left atrium, is swept to the periphery, or rupture of an atherosclerotic plaque inside the coronary vessel) no blood can reach the tissue beyond this point if there is no other vessel distributing to the same region. This state is called ischemia. The most affecting factor is the absence of oxygen supply, resulting in hypoxia. Energy formation in myocardial cells is driven by oxygenation of free fatty acids. Upon hypoxia, anaerobic energy formation fills the gap until the environment is saturated with lactic acid. The most important cellular energy transporter is the molecule ATP (adenosinetriphosphate). Energy dependent processes, as for example the maintenance of ionic gradients across cell membranes will stop on depletion of ATP. Change of ionic composition inside cells is a major contributor to the initiation of cellular necrosis processes. Autolysis takes place by activation of intracellular enzymes, and decomposition of cell membranes. Intracellular proteins (myoglobin, troponin) leak through defect endothelia and can be detected in the blood.⁴¹ Research on the accuracy and standardization of these biochemical markers of myocardial infarction has been very prodigious in the last ten years and it has been addressed as a cover topic in journals dealing with clinical chemistry.⁴² The search for more specific, sensitive, and immediately responding serum markers is still going on.⁴³ Myoglobin can already be detected 2 – 6 hours after a coronary occlusion, but it is not specific to the heart, since it exists also in skeletal muscle cells. Troponin can be detected later but has a heart specific isoform, which can be distinguished with the proper antibodies (in this case patented by Hoffmann-La Roche). CRP is a general indicator of inflammatory processes (see the following section). D-dimers are a standard indicator for blood clotting processes in the past few hours. They are a cleavage product of fibrin and could be used as a sensitive but not specific marker for exclusion of pneumonic embolism, which can present the same symptoms as AMI.

2.8 Contact Angle Goniometry

Contact angle goniometry is a technique to evaluate the wetting properties of a substrate by measuring the angle of the shape profile of a drop that is formed by a liquid on a surface of interest. If the liquid does not wet the surface

³⁸ Patrick L, Uzick M. Cardiovascular disease: C-reactive protein and the inflammatory disease paradigm: HMG-CoA reductase inhibitors, alpha-tocopherol, red yeast rice, and olive oil polyphenols. A review of the literature. Altern Med Rev. 2001; 3, 248.

³⁹ Roberts WL, Moulton L, Law TC, Farrow G, Cooper-Anderson M, Savory J, Rifai J. Evaluation of nine automated high-sensitivity C-reactive protein methods: implications for clinical and epidemiological applications. Part 2. Clin Chem. 2001; 3, 418.

⁴⁰ Stenman UH. Immunoassay standardization: Is it possible, who is responsible, who is capable? Clin Chem. 2001; 47, 815.

⁴¹ Mair J. Tissue release of cardiac markers: from physiology to clinical applications. Clin Chem Lab Med. 1999; 37 (11/12), 1077.

⁴² Clin Chem Lab Med 1999; 37(11/12).

⁴³ Christenson RH, Azzazy HME. Biochemical markers of the acute coronary syndrome. Clin Chem. 1998; 8(B), 1855.

completely ($\Theta = 0$) one can measure an angle, which is termed the angle of contact. The equilibrium of such systems can be described by Young's equation. The experimental setting used for this work measures angles of captive drops. A small volume of liquid is placed on the surface, the advancing contact angle Θ_a is measured, a portion of this volume is aspirated again and the receding contact angle Θ_r is measured. The difference $\Delta \cos(\Theta) = \cos(\Theta_r) - \cos(\Theta_a)$ is termed hysteresis and is an important indicator for the homogeneity of the surface.⁴⁴

2.9 X-Ray Photoelectron Spectroscopy

X-Ray photoelectron spectroscopy (XPS) is a convenient method for a precise investigation of the chemical composition of surfaces.⁴⁵ This method relies on the ejection of electrons from surface atoms by X-rays (photons with high energy).

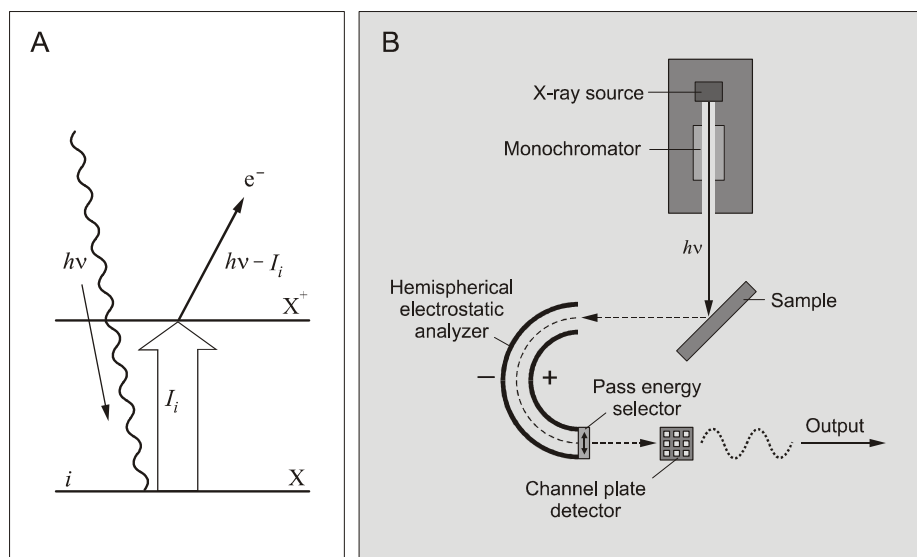


Figure 6. Principle of photoelectron spectroscopy. (A) An incoming photon ejects an electron from its orbital. (B) Basic components of an XPS and their arrangement. [fig. by M. Geissler]

Electrons ejected by the photoelectric effect are called photoelectrons. The kinetic energy E_{kin} of the photoelectrons corresponds to the difference between the energy $h\nu$ of the incoming X-ray photons and the ionization energy I_i , which is required to remove an electron from the orbital i of an atom. This correlation can be expressed by the following equation,

$$(3) \quad E_{kin} = h\nu - I_i$$

where h is Planck's constant, and ν is the frequency of the X-rays. In XPS, the kinetic energy of the photoelectrons is measured: for a given energy of the photons, the detected kinetic energies of the photoelectrons can be used to calculate the core level binding energies (corresponding to I_i) of an atom. The

⁴⁴ Ulman A. An introduction to ultrathin organic films. 1991, pp48. Academic Press, San Diego, CA, USA.

⁴⁵ Carson TA. Photoelectron and Auger Spectroscopy, Plenum Publishing Co, New York, USA, 1975.

atomic identification of elements is possible with this method, because every element has a specific set of core levels and binding energies. Changes in the oxidation state of an element affect local binding energy states, which results in “chemical” shifts of the kinetic energy of the photoelectrons. This effect can provide useful information about the chemical environment of an element.⁴⁶ In principle, the quantification of a measurement is possible by using peak area and peak height sensitivity factors which have been established for individual signals of several elements. XPS measurements are performed in ultra-high vacuum (UHV) at a pressure of $\sim 10^{-9}$ mbar and they usually require a complex and expensive setup. A simplified scheme of an X-ray photoelectron spectrometer is shown in Figure 6. A monochromatized beam of photons produced in the X-ray source (often used is an AlK α source, $E = 1486.6$ eV) interacts with the sample. The photoelectrons ejected from the sample are collected as a function of their kinetic energy by a hemispherical analyzer. The pass-energy selector terminating the analyzer modulates the energy dispersion around a selected energy (which mainly determines the resolution and the sensitivity of a measurement). A channel plate detector finally transforms the electronic flow into signals, which can be digitized and converted into a spectrum.

2.10 Ellipsometry

Ellipsometry is a fast and inexpensive method to characterize films thinner than 15 nm on a supporting substrate and to determine their thickness. Plane-polarized light impinges at a defined angle of incidence on the surface of a substrate (Figure 7). The reflected beam is elliptically polarized. The ratio of amplitudes of the two components of the light together with its phase shift are related to the thickness t_s and the complex refractive index ($N_s = n_s + k_s i$) of the substrate. A thin film deposited on the substrate changes the reflected polarized light depending on the refractive index n_f and the thickness t_f of the film. As it is not possible to determine both refractive index and thickness simultaneously, values of the refractive index of such films are set or assessed beforehand.⁴⁷ For protein layers, n_f is estimated to be 1.45 at 645 nm. Ellipsometry can be used to measure accurately biomolecule layers on reflective supports and to detect binding events on these molecules by measuring the change in thickness.⁴⁸ A 0.05 increase of n_f induces a 0.1 nm decrease of the calculated thickness. Ultrasensitive immunoassays for hepatitis B surface antigen and alpha-fetoprotein using this principle have been constructed.⁴⁹

⁴⁶ Egelhoff WF. Surf Sci Rep. 1987; 6, 253.

⁴⁷ Azzam RMR, Bashara NM. Ellipsometry and polarized light. North Holland, Amsterdam, 1977.

⁴⁸ Striebel C, Brecht A, Gauglitz G. Characterization of biomembranes by spectral ellipsometry, surface plasmon resonance and interferometry with regard to biosensor application. Biosens Bioelectr. 1994; 9, 139.

⁴⁹ Ostroff RM, Maul D, Bogart GR, Yang S, Christian J, Hopkins D, Clark D, Trotter B, Moddel G. Fixed polarizer ellipsometry for simple and sensitive detection of thin films generated by specific molecular interactions: applications in immunoassays and DNA sequence detection. Clin Chem. 1998; 9, 2031.

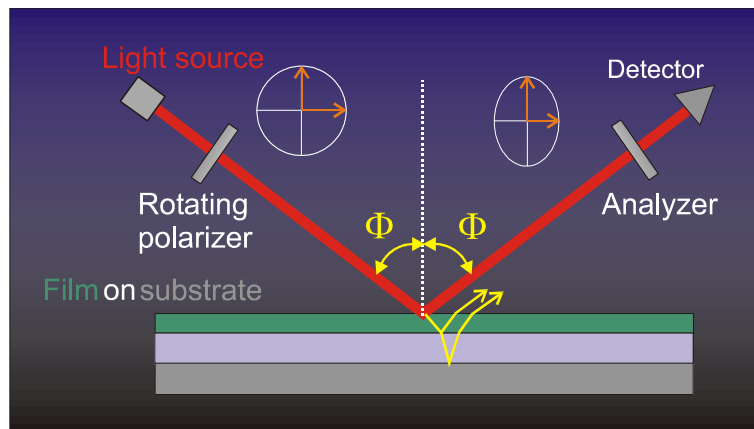


Figure 7. In Ellipsometry, a laser beam is reflected on the substrate. [fig. by A. Bernard]

2.11 Affinity Chromatography

In conventional liquid chromatography, unspecific chemical interactions due to physical properties of the passing molecules (size, charge, polarity) induce different retention times, which induce the separating process.⁵⁰ Affinity chromatography, in contrast is based on the specific interaction between a target molecule and a solid phase ligand (Figure 8). If desired, elution of the bound analyte can be achieved by rinsing with low pH or high ionic strength, depending on the nature or the binding.

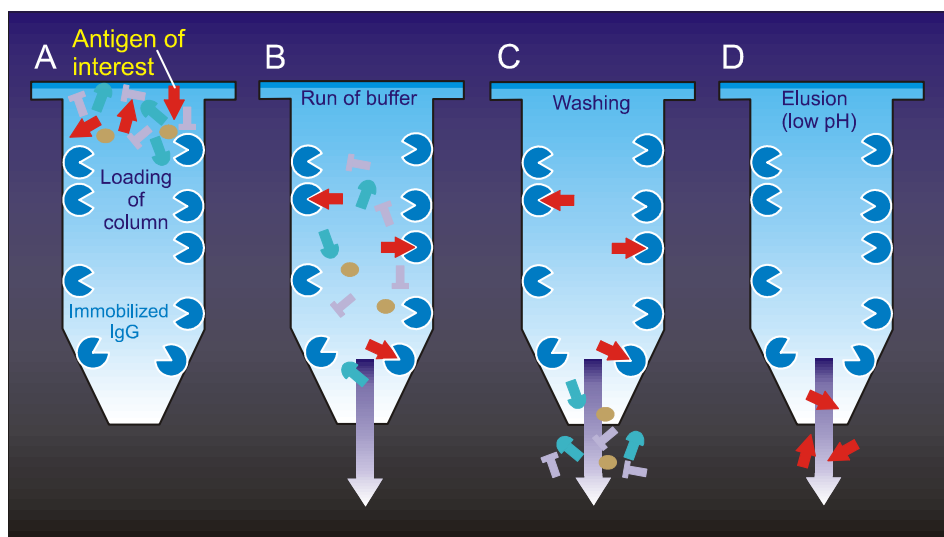


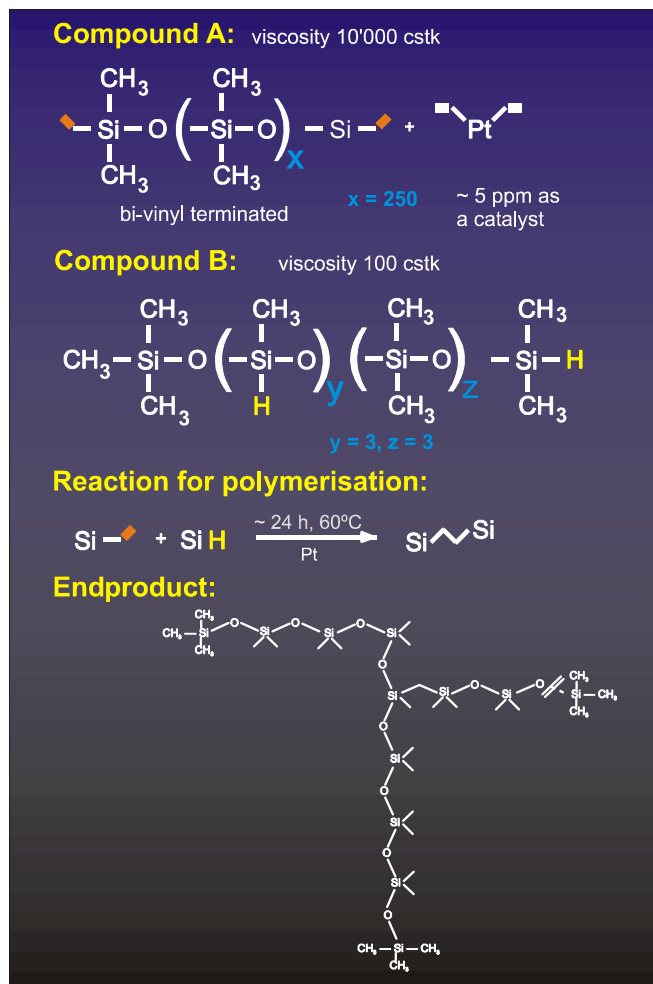
Figure 8. A specific binding behaviour is used in affinity chromatography. [fig. by A. Bernard]

2.12 Polydimethylsiloxane

Poly(dimethylsiloxane) (PDMS) can be polymerized from its precursors either thermally with a platinum catalyst or under UV light with a radical initiator. Figure 9 outlines the chemistry of the polymerization process. The principle characteristics of PDMS are listed in Table 1.

⁵⁰ Porath JJ. Metal-ion hydrophobic, thiophilic and II-electron governed interactions and their applications to salt-promoted protein adsorption chromatography. Biotechnol Progress. 1987; 3, 14.

-
- Forms conformal contact
 - Deformable
 - Low interfacial free energy: $21.6 \cdot 10^{-3} \text{ Jm}^{-2}$
 - Chemically inert
 - Homogeneous, isotropic, optically transparent ($< 300 \text{ nm}$)
 - Durable
 - Surface derivatization possible (O₂-Plasma, SAM)
-

Table 1. Some properties of PDMS.⁵¹**Figure 9.** Reaction educts and polymerization reaction of poly(dimethyl)siloxane (PDMS). [fig. by A. Bernard]

2.13 Self-Assembled Monolayers of Thiols on Gold

Self-assembled monolayers (SAMs) can be formed by immersion of a gold surface into a solution of alkanethiols and have been well characterized.^{52,53,54}

⁵¹ Xia Y, Whitesides GM. Soft Lithography. Angew Chem Int Ed Engl. 1998; 37, 550.

⁵² Bain CD, Troughton EB, Tao YT, Evall J, Whitesides GM, Nuzzo RG. Formation of monolayer films by spontaneous assembly of organic thiols from solution onto gold. J Am Chem Soc. 1989; 111, 321.

⁵³ Delamarche 1994 SAMs

⁵⁴ Delamarche E, Michel B, Kang H, Gerber C. Golden interfaces: The surface of self-assembled monolayers. Adv Mat. 1996a; 8, 719.

Formation of the monolayers occurs by chemisorption of the sulphur atom to the gold surface with high affinity and stability (Au-S: $dG \sim 40 \text{ kcal mol}^{-1}$, half the value of a C-C bond).⁵⁵ Figure 10 shows the tilted arrangement of the alkane chains on the surface.

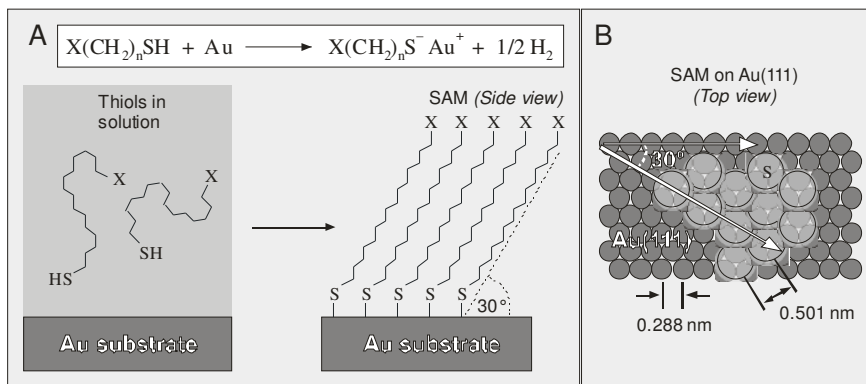


Figure 10. (A) Single thiol molecules are twisted in solution. Upon adsorption on gold, a regular, tilted arrangement appears. (B) The areal density of the thiol molecules in comparison with the atomic view of the gold surface. [fig. by M. Geissler]

Different terminating groups of the alkanethiols allow formation of monolayers with varying chemical and physical properties (e.g. wettability). A topic of major interest is the generation of biocompatible surfaces (implants, food industry, ship construction).⁵⁶ Monolayers of alkanethiols with a whole spectrum of different ω -groups have been investigated on their wettability and resistance to adsorption of proteins and detergents.^{57,58,59,60} Efforts were made to relate protein and detergent adsorption on thiol-SAMs to the surface wettability of the SAMs.⁶¹ Mobility and aggregation of proteins and their interaction with SAMs also depend strongly on the chain length of the bound alkane chains.⁶² Polyethyleneglycol resists the adsorption of proteins.^{63,64,65}

⁵⁵ Whitesides GM, Laibinis PE. Wet chemical approaches to the characterization of organic surfaces: Self-assembled monolayers, wetting, and the physical-organic chemistry of the solid-liquid interface. *Langmuir*. 1990; 6, 87.

⁵⁶ Chapman RG, Ostuni E, Liang MN, Meluleni G, Kim E, Yan L, Pier G, Warren HS, Whitesides GM. Polymeric thin films that resist the adsorption of proteins and the adhesion of bacteria. *Langmuir*. 2001; 17, 1225.

⁵⁷ Sigal GB, Mrksich M, Whitesides GM. Using surface plasmon resonance spectroscopy to measure the association of detergents with self-assembled monolayers of hexadecanethioate on gold. *Langmuir*. 1997; 13, 2749.

⁵⁸ Chapman RG, Ostuni E, Yan L, Whiteside GM. Preparation of mixed self-assembled monolayers (SAMs) that resist adsorption of proteins using the reaction of amines with a SAM that presents interchain carboxylic anhydride groups. *Langmuir*. 2000a; 16, 6927.

⁵⁹ Holmlin RE, Chen X, Chapman RG, Takayama S, Whitesides GM. Zwitterionic SAMs that resist nonspecific adsorption of protein from aqueous buffer. *Langmuir*. 2001; 17, 2841.

⁶⁰ Chapman RG, Ostuni E, Takayama S, Holmlin RE, Yan L, Whitesides GM. Surveying for surfaces that resist the adsorption of proteins. *J Am Chem Soc*. 2000b; 122, 8303.

⁶¹ Sigal GB, Mrksich M, Whitesides GM. Effect of surface wettability on the adsorption of proteins and detergents. *J Am Chem Soc*. 1998; 120, 3464.

⁶² Yang Z, Galloway JA, Yu H. Protein interactions with poly(ethylene glycol) self-assembled monolayers on glass substrates: diffusion and adsorption. *Langmuir*. 1999; 15, 8405.

⁶³ Bailey FE, Koleske Jy. *Poly(Ethylene Oxide)*, Academic Press, New York, 1976.

⁶⁴ Harris JM, Zalipsky S. *Poly(ethylene glycol)*. Chemistry and Biological Applications. American Chemical Society, Washington DC, 1997.

and of many detergents.⁵⁷ A simple method to print alkanethiols on gold surfaces with a stamp of PDMS was developed, which allows structured derivatization of gold surfaces.^{66,67}

Thiol-SAMs on gold thus provide a means to define surface properties like contact angle and control of protein adsorption in a well-defined and structured manner.⁶⁸

⁶⁵ DiMilla P, Folkers JP, Biebuyck HA, Harter R, Lopez G, Whitesides GM. *J Am Chem Soc.* 1994; 116, 2225.

⁶⁶ Delamarche E, Schmid H, Bietsch A, Larsen NB, Rothuizen H, Michel B, Biebuyck H. Transport mechanisms of Alkanethiols during microcontact printing on gold. *J Phys Chem B.* 1998; 102, 3324.

⁶⁷ Libioulle L, Bietsch A, Schmid H, Michel B, Delamarche E. Contact-inking stamps for microcontact printing of alkanethiols on gold. *Langmuir.* 1999; 15, 300.

⁶⁸ Delamarche E, Sundarababu G, Biebuyck H, Michel B, Gerber C, Sigrist H, Wolf H, Ringsdorf H, Xanthopoulos, Mathieu HJ. Immobilization of antibodies on a photoactive self-assembled monolayer on gold. *Langmuir.* 1996b; 12, 1997.

3 EXPERIMENTAL SECTION

3.1 Solid Phase Substrate

PDMS serves as the solid phase substrate and it was obtained by curing the prepolymer components of Sylgard 184 (Dow Corning, Midland, MI) at 60° C for at least 24 h between the bottom of a polystyrene dish and a plan parallel flat piece of glass. Subsequently the substrate was cut to the desired dimensions ($2 \times 3 \text{ mm}^2$).

3.2 Fabrication of Microfluidic Networks

Standard photolithography was used to pattern microchannels and pads in Si wafers. The wafers were first spin-coated at 4000 rpm with ~1.2 μm of AZ6612/H₂O (1:4; Hoechst), photoexposed through a Cr mask (Photronics, Dresden, Germany) and developed for 30 s in AZ400/H₂O (1:4; Hoechst). The photoresist acted as a mask for an inductively coupled plasma (reactive ion etcher from Surface Technology Systems, Cambridge, U.K.) to pattern the silicon wafer. The geometry of the μ FN consisted of sixteen $1.5 \times 1.5 \text{ mm}^2$ pads connected by eight 20 μm wide channels. Channels and pads both had a depth of 20 μm .

3.3 Surface Preparation of the Silicon Wafer

The silicon wafers were put under a UV lamp (UV-Ozone Photoreactor PR-100, Ultra-Violet Products, Upland, CA) for 15 min and rinsed with Ethanol. A flat piece of PDMS, sufficiently large to cover the wafer with the μ FNs, was rinsed with Ethanol for 2 s and was dried under a stream of N₂. A sufficient amount of 0.3 mM solution of Eicosanethiol (Robinson Brothers, West Bromwich, West Midlands, US) in Ethanol to cover entirely the PDMS surface was deposited for at least 30 s (Figure 11A). The substrate was then dried under N₂ and put on the wafer for at least 20 s to allow establishment of conformal contact (Figure 11B). Thus, formation of a hydrophobic Au-ECT SAM sparing the channels and pads was formed (Figure 11C). Covering the channels with a hydrophilic layer of PEGs was achieved by immersion of the μ FNs in a 10 mM solution of a Poly(ethylene)glycol with the structural formula of CH₃O-POE_x-NH-CO(CH₂)₂-SH (Rapp Polymere, Tuebingen, Germany) in Ethanol (Figure 11D). The functionalized wafer is wettable inside the channels (PEG) and pads and non-wetting on the surrounding surface (ECT), Figure 11E.

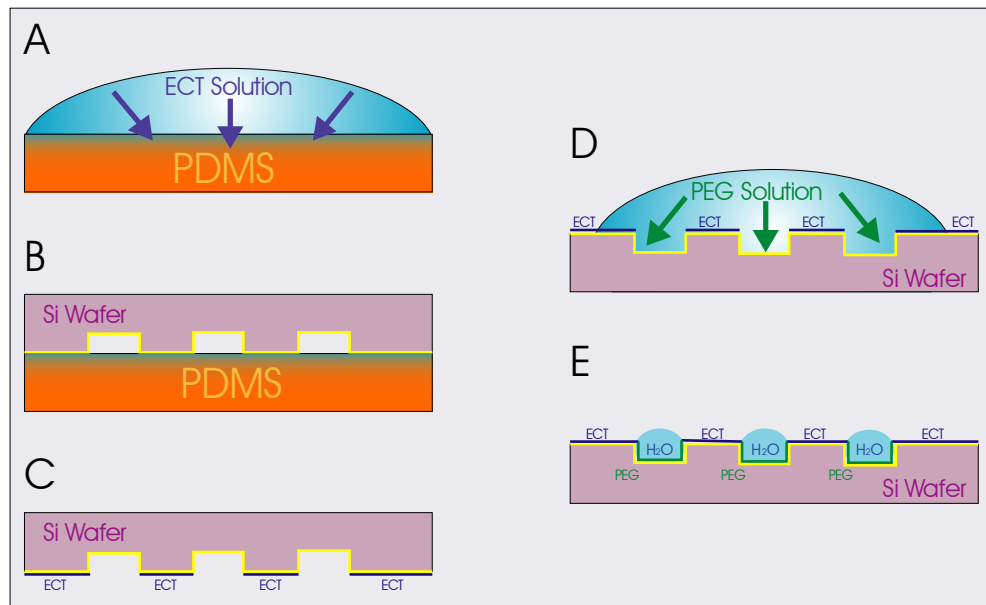


Figure 11. Production of wetting channels and repelling surroundings. (A) A flat piece of PDMS is incubated with a solution of Eicosanethiol (ECT). (B) The gold coated wafer with the capillary structure is put on this piece of PDMS. The ECT molecules are thus selectively printed on the channel spacing. (C) The resulting monolayer of ECT on the wafer. (D) The wafer is incubated with a solution of poly(ethylene)glycol (PEG). The PEG molecules adsorb preferentially on the ECT-free gold surface. (E) The resulting thiol monolayer pattern with regionally differing wetting properties.

3.4 Surface Characterization of the Silicon Wafer

XPS spectra were acquired on a Sigma Probe VG Scientific spectrophotometer operation at a base pressure of $\leq 10^{-9}$ mbar and equipped with a monochromatized Al K α source ($E = 1486.6$ eV). The X-ray spot was focused down to 400 μm in diameter. The analyzer had an angle of 37° to the sample. Samples were mounted on a multisample holder stage for examination under the same conditions. Spectra are referenced to the Au 4f_{5/2} peak at 84 eV. For all samples survey spectra were acquired first with a pass energy of 80 eV (0.4 eV steps for 40 ms) and high-resolution spectra for N 1s, O1s, C1s were taken with a pass energy of 40 eV (0.05 eV steps for 100 ms). The electron beam used to generate the X-rays had in all cases an intensity of 13 mA, which remained stable within <5% during the experiments. The intensity of the peaks from the substrates did not vary noticeably during the experiments, which indicated no particular damages on the surfaces of the grafted samples during the measurements.

Wettability of the modified surfaces by water was determined using a Kruess contact angle goniometer (Hamburg, Germany) equipped with a motorized pipette (Matrix Technology, Nashua, NH). Advancing and receding angles were measured at multiple distinct locations on each sample.

Ellipsometry was used to measure the change in monolayer coverage of the gold samples. For this purpose, a Rudolph AutoEL automatic thin-film ellipsometer equipped with a 632.9 nm He-Ne laser and operating at an angle of incidence of 70° has been used. The polarizer angle was 45°. The complex refractive index of the gold substrate, $N_s = n_s + k_s i$, was measured first. The thickness of the SAMs was measured at precise locations ($\Delta < 0.5$ mm), where n_s and k_s were recorded. The instrument was calibrated by measuring a series

of SAMs of alkanethiols ($\text{CH}_3(\text{CH}_2)_{n-1}\text{SH}$, $n = 2, 4, 6, 8, 12, 14, 16, 18, 20$) on Au having known thicknesses. For this series of thiols a refractive index of $n_f = 1.45$ was used. The accuracy was ± 0.1 nm using this method.

3.5 Chemicals and Biochemicals

Ethanol (Fluka Chemie, Buchs, Switzerland) was used. When stated dH_2O it stands for deionised water purified with a Millipore Simplicity 185 (Millipore S.A., Molsheim, France) filtering device with purity grade of $18.2 \text{ M}\Omega$ was used. Drying under a stream of N_2 was performed using gas emanating from liquid N_2 .

Prepacked phosphate buffered saline (PBS) from Pierce Chemicals (Rockford, IL) with pH 7.2, 0.1 M sodium phosphate and 0.15 M sodium chloride was prepared with Millipore H_2O . Bovine serum albumin, BSA (Sigma Chemicals, St. Louis, MO) was diluted in PBS to a working concentration of 10 mg mL^{-1} . Human blood was extruded with S-Monovettes (Sarstedt) containing Li-Heparin for a final concentration of 15 IE mL^{-1} of blood. The plasma fraction was separated by double centrifugation at 5500 rpm for 10 min equivalent to a force of 2000 times earths gravity (Eppendorf Centrifuge 5415 D). Monoclonal antibodies αhCRP (mouse IgG1, clone C2) αhCRP FITC conjugate (mouse IgG2a, clone C6), anti-human cardiac myoglobin (mouse IgG1, clone 7C3), anti-human cardiac myoglobin FITC conjugate (mouse IgG1, clone) and antigens CRP, myoglobin used were obtained in PBS solution with 0.1 % sodium azide as a preservative (Hytest, Turku, Finland). For affinity purification of human plasma 10 mg of protein A coated sepharose (Sigma Chemical, St. Louis, MO) were incubated for one hour at room temperature on a shaker with $200 \mu\text{L}$ of a solution of rabbit polyclonal αCRP which was obtained in lyophilized form (Anawa Trading, Wangen, Switzerland) and diluted in 1 mL PBS following the manufacturers recommendations. Separation of unbound immunoglobulins was accomplished by repeated centrifugation for 2.5 min at 13200 rpm, discarding of fluid fraction and redistribution in PBS on a vortex for at least seven times. The functionalized sepharose was incubated with 1 mL of human plasma for one hour at room temperature on a shaker and eventually separated again by centrifugation. Human plasma did not produce a signal that was discernable from the background signal in microfluidic immunoassays.

3.6 Image Acquisition

Images were acquired with a ST-8 CCD (SBIG, Santa Barbara, CA) mounted on an epifluorescence microscope (Nikon Labophot-2) with a filter set consisting of 465 - 495 nm excitation, 505 nm dichroic mirror and 515 - 555 nm emission (Nikon FITC) and a xenon arc lamp (Osram, XBO 100W OFR). Skypro software (Software Bisque, Golden, CO) was used for data acquisition and visualization. Exposure integration time was 16 s with 4 fold attenuation by insertion of a neutral density filter into the excitation path. Quantitative analysis was performed with a program written in LabView by Bruno Michel. Inhomogenous illumination field and substrate autofluorescence was accounted for as in,

$$s = \frac{s^* - b}{a - b} \quad (6)$$

where s^* is the raw signal data, b the constant background (introduced by SkyPro software and physically by external stray light) and a the autofluorescence signal of the substrate, obtained by measurement. Calculations are averaged on spots of 16 x 16 pixels as standard deviation is kept lower thus than with pixel by pixel operation. The data was graphically interpreted with Origin 6.0 (Microcal).

4 RESULTS

4.1 Patterned Delivery of Proteins with Microfluidic Networks

By putting a flat substrate of PDMS on top of a capillary network in silicon, small capillaries are formed. Width and depth of the capillaries used for our experiments in this work were $20 \times 20 \mu\text{m}^2$. The driving forces to fill the capillaries are solely capillary forces. Filling with solutions of proteins enables accurate delivery to specific regions on the substrate surface and has already been described.^{69,70} Application of this technique to produce immunoassays has been demonstrated.⁷¹ The basic principle of combinatorial microfluidic immunoassays, the micromosaic immunoassays, is shown in Figure 12.

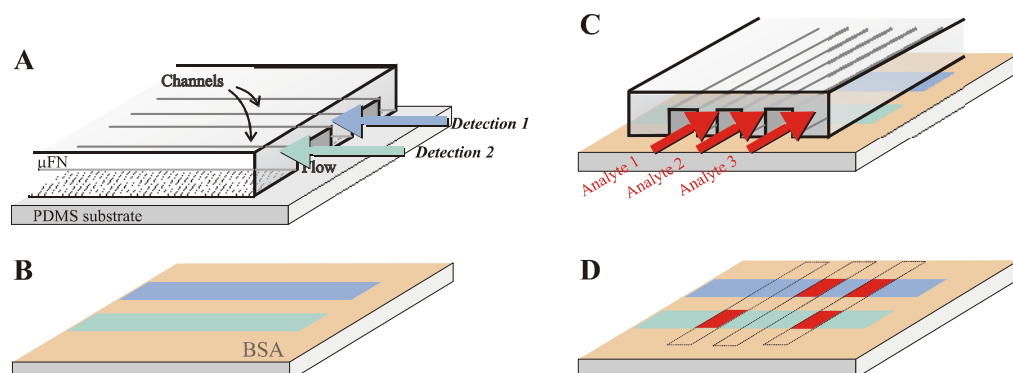


Figure 12. Patterning surfaces with proteins using microfluidic networks. (A) The element with the channels are put on top of a flat substrate. The resulting capillaries are filled with capture antibody solution. The proteins adsorb to the substrate surface. The channels are flushed with a blocking solution (BSA). (B) The element is taken away and the entire substrate is blocked. (C) The element is put on the substrate, with the channels orthogonal to the direction they had in the first step. Samples are introduced into channels and analyte binds to capture antibody. Channels are rinsed with blocking solution. Detection antibody solution is filled in. Channels are rinsed again with blocking solution. (D) The microfluidic network is taken off, and fluorescence microscopy reveals a pattern which can be analysed. [fig. by A. Bernard]

A typical pattern of fluorescent microspots is produced with a μ MIA and can be detected with a fluorescence microscope (Figure 13).

⁶⁹ Delamarche E, Bernard A, Schmid H, Bietsch A, Michel B, Biebuyck H. Microfluidic Networks for chemical patterning of substrates: design and application to bioassays. *J Am Chem Soc.* 1998; 120, 500.

⁷⁰ Juncker D, Schmid H, Bernard A, Caelen I, Michel B, de Rooij N, Delamarche E. Soft and rigid two-level microfluidic networks for patterning surfaces. *J Micromech Microeng.* 2001; 11, 532.

⁷¹ Bernard A, Michel B, Delamarche E. Micromosaic Immunoassays. *Anal Chem.* 2001; 73, 8.

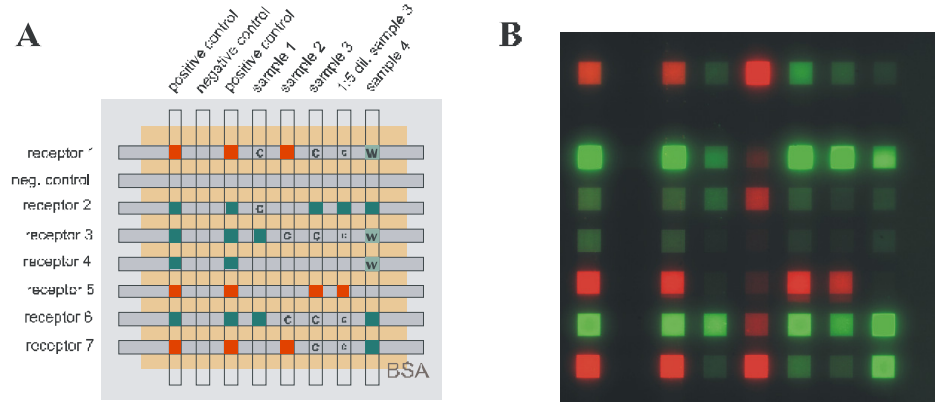


Figure 13. Different solutions can be inserted into the 8 individual channels. Thus, a maximum of 64 single fluorescent spots can be obtained. (A) Schematized representation of the resulting pattern of a micromosaic immunoassay. (B) Picture obtained by fluorescence microscopy of a micromosaic pattern. The two different colours represent different signals of two different tags on the same substrate, whose signal has been superimposed in this picture. [fig. from ref. 71]

A flow promoting sheet of nylon put atop the exit pads of the microfluidic network can soak up the liquids from the exit pads. Thus, the entire volume of liquid filled into the loading pads passes through the microchannels. The loading pads become empty again and they can be refilled with a different liquid without removal of the PDMS substrate (Figure 14).

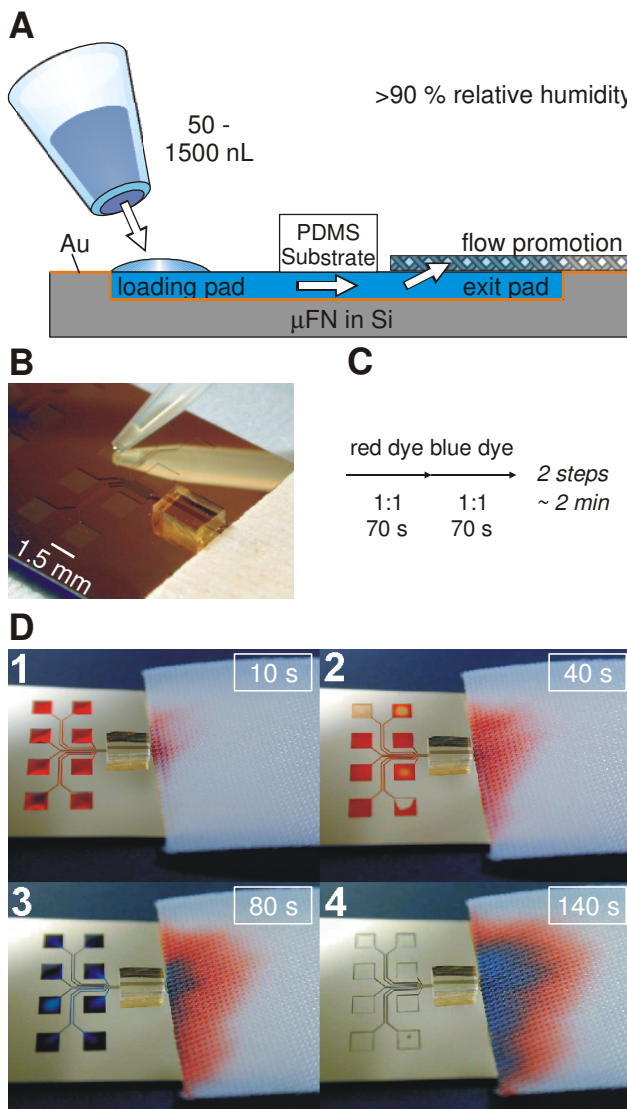


Figure 14. Method for exposing a PDMS substrate to solutions using a μ FN. (A) A solution placed on the pad of a microfabricated μ FN flows through the microchannel and into a flow-promoting structure because of capillary forces. (B) This photograph shows a block of PDMS placed over the microchannels of the μ FN, which serves as the substrate for the immunoassays performed in this work. (C) Loading solutions consecutively into the same pad is denoted throughout this publication with arrows: Each arrow corresponds to an elementary step (filling, rinsing, blocking, etc.); compounds in the solution are indicated above the arrow, their concentration and the duration of the step below. Here, the two arrows refer to (D), in which all eight independent pads are loaded sequentially with a red and a blue solution. The absorbing tissue after the PDMS block provides both the capillary pump and waste element of the μ FN.

4.2 Working Procedure of a Micromosaic Immunoassay

The 8 channels of a freshly prepared μ FN were covered with a piece of PDMS. A humidity chamber was set up, containing a heater plate constantly keeping a beaker with water at a temperature around 65 °C to generate a relative humidity varying between 85 and 95 %. The channels of the μ FN were filled and rinsed in this ambient in order to keep evaporation at a minimum level. First, 100 μ L of PBS were placed on one side of substrate and were allowed to fill the channels. A piece of clean room paper with strong soaking capability was placed on the drop. The paper adhered to the surface by wetting

forces. On the opposite side 500 nL of capture antibody solution in PBS were filled separately into the filling pads. After one minute, 500 nL of BSA were added in each pad and allowed to flow for 30 s. All the filling pads were then flushed at once with 200 µL of BSA from a pipette and the substrate was taken off. Then the substrate was rinsed with Millipore water for 3 s and placed on a fresh µFN with the deposited lines of proteins orthogonal to the channels of the wafer. 100 µL of BSA solution were placed on the exit pads and a piece of clean room paper was placed on top of this drop. 500 nL of sample solution were filled into the loading pads and were allowed to flow for 2 minutes. 500 nL of BSA were then added in each pad and were left flowing for 30 s. The area of the loading pads was rinsed with a stream of BSA (1 – 2 mL) from a syringe. 5 µL of detection antibodies solution were placed over the loading channels for 2 minutes. The loading channels and pads were rinsed with a stream of BSA. The BSA was left in the loading pads for 30 s. The substrate was taken off and was rinsed 3 s with Millipore water. It was put on a glass slide and was covered with a glass cover sheet (0.17 mm thickness), which allowed image acquisition with the fluorescence microscope. An overview of the single steps is given in Figure 15.

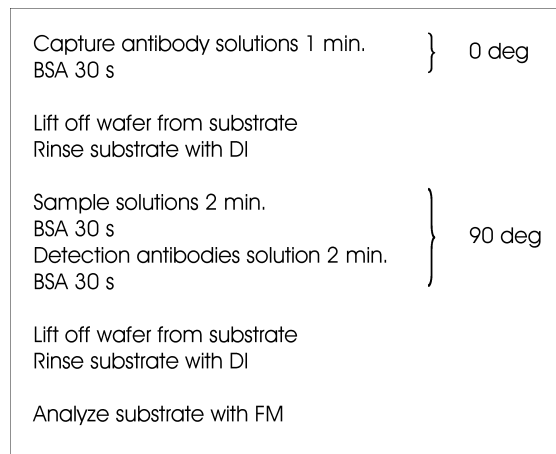


Figure 15. The sequence steps of the micromosaic immunoassay. BSA: bovine serum albumin, DI: deionized water, FM: fluorescence microscope.

4.3 Optimization of the Wafer Surface

To assess the optimal time necessary for the PEG molecules to form a continuous monolayer we immersed pieces of silicon wafers covered with a 50 nm thick layer of Au by in a solution of PEG in Ethanol. In order to keep incubation time low we chose a concentration of 10 mM, which is ten times higher than the commonly used concentrations.⁵⁵ After an immersion time of 1 s, 5 s, 10 s, 30 s, 60 s, 5 min, 10 min, 13 min, respectively, we characterized the newly formed monolayer by ellipsometry and contact angle determination. For the graphical interpretation of the ellipsometrical data we chose $n_f = 1.45$ as refractive index of the monolayer in order to calculate its approximate thickness.

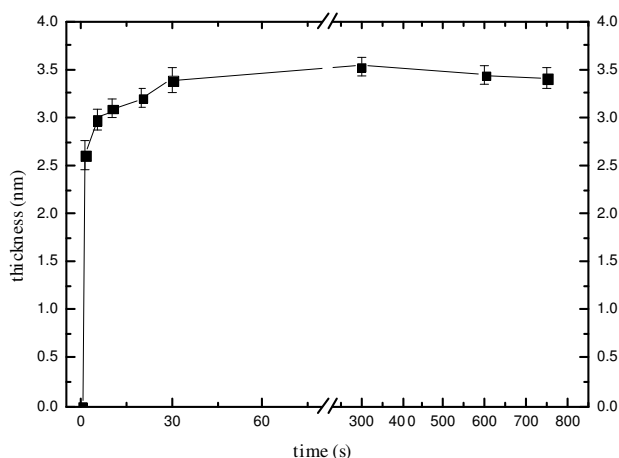


Figure 16. Formation of a PEG-thiol monolayer on a gold surface upon immersion in a 10 mM solution of PEG-thiols in EtOH. The thickness of a PEG-thiol layer reaches its saturation level of 3.3 nm already after immersion times of ~30 s. This value agrees with the values of complete layers... . Completeness of the PEG-thiol monolayer ensures protein repellency and favorable wetting properties of the derivatized gold surface. The thickness of the PEG-thiol monolayer has been calculated from ellipsometrical data using a refractive index $n_f = 1.45$.

As anticipated, the curve in Figure 16 exhibits the characteristic slope of a saturation behaviour termed Langmuir isotherm,^{72,73} where the desired properties of contact angles and layer thickness are clearly attained already after a few seconds. For our purposes it was important to have contact angles of the PEG monolayer as low as possible (in order to provide rapid filling), and a complete monolayer (indicated by its thickness). Complete monolayers are important to prevent protein physisorption to uncovered areas of Au. A second criterion is the wettability of the surface to provide proper filling of the channels. The advancing and receding contact angles of the PEG monolayers have been measured six times each one. The angles were $\Theta_a = 45.2$, $\Theta_r = 38.8$, and $\Theta_a = 44.2$, $\Theta_r = 38.7$ for immersion times of 30 s and 10 min respectively. There was no significant difference in the contact angles of 30 s and 10 min immersion time. An immersion time of 30 s in a solution of 10 mM PEG-thiols in ethanol is thus sufficient to form a homogenous monolayer of PEG-thiols on gold.

When inking a PDMS stamp with thiols and consequently printing it onto a surface of Au the layer is usually not form as completely as if it were formed by immersion in the corresponding solution of thiols in Ethanol.⁷⁴ Due to this phenomenon, we wanted to investigate the chemical composition of the ECT monolayers in the immediate neighbourhood of the filling pads and channels of the μ FNs, where completion of the imperfect monolayer of ECT by molecules of PEG could occur during incubation with PEG solution. X-ray photospectroscopy is ideal, because statements about the occurrence of

⁷² Langmuir I. J Am Chem Soc. 1917; 39, 1848.

⁷³ Berger R, Delamarche E, Lang HP, Gerber C, Gimzewski JK, Meyer E, Guentherodt HJ. Surface stress in the self-assembly of alkanethiols on gold. Science. 1997; 276, 2021.

⁷⁴ Larsen NB, Biebuyck H, Delamarche E, Michel B. Order in microcontact printed self-assembled monolayers. J Am Chem Soc. 1997; 119, 3017.

specific isotopes can be made. We measured two individual spots on the same piece of wafer, one in a filling pad with a PEG monolayer, another one in a distance of 1.5 mm from the border of the filling pad onto where the ECT had been printed.

The X-ray beam was focused to 400 μm . The XPS survey corresponding to the derivatization of the fluidic zones with HS-PEG revealed the presence of O 1s at 532 eV and two peaks of C 1s at 287.5 eV. The Au 5f_{1/2} centred at 84 eV corresponds to the Au surface underneath the monolayer. The sulphur of the HS-PEG molecule, expected at 163 eV, was not visible due to its high attenuation by PEG-chain composing the rest of the monolayer. The intensities of the O 1s and C 1s peaks were as expected for a poly(ethylene) chain.⁷⁵ The high-resolution spectrum of the C 1s for this surface, revealed only 3% of contaminants in the HS-PEG layer indicating that the HS-PEG layer is of very high purity. The spectrum obtained next to the filling pad corresponding to the region where HS-ECT was microcontact printed revealed 1 type of carbon at 285 eV and a minor unexpected peak of oxygen at 532 eV. The carbon signal corresponds to the alkyl chain of the HS-ECT monolayer and the small oxygen signal to the oxygen present in the HS-PEG molecules. These HS-PEG molecules were included during the derivatization step of the inside the microchannels. Such an insertion is known and has been extensively reported.⁷⁶ Importantly, the inclusion of some HS-PEG molecules in the HS-ECT monolayer did not compromise the hydrophobic properties of the HS-ECT monolayer (Figure 17).

⁷⁵ Pale-Grosdemange C, Simon ES, Prime KL, Whitesides GM. J Am Chem Soc. 1991; 113, 12.

⁷⁶ Bain CD, Evall J, Whitesides GM. Formation of monolayers by the coadsorption of thiols on gold: variation in the head group, tail group, and solvent. J Am Chem Soc. 1989; 111, 7155.

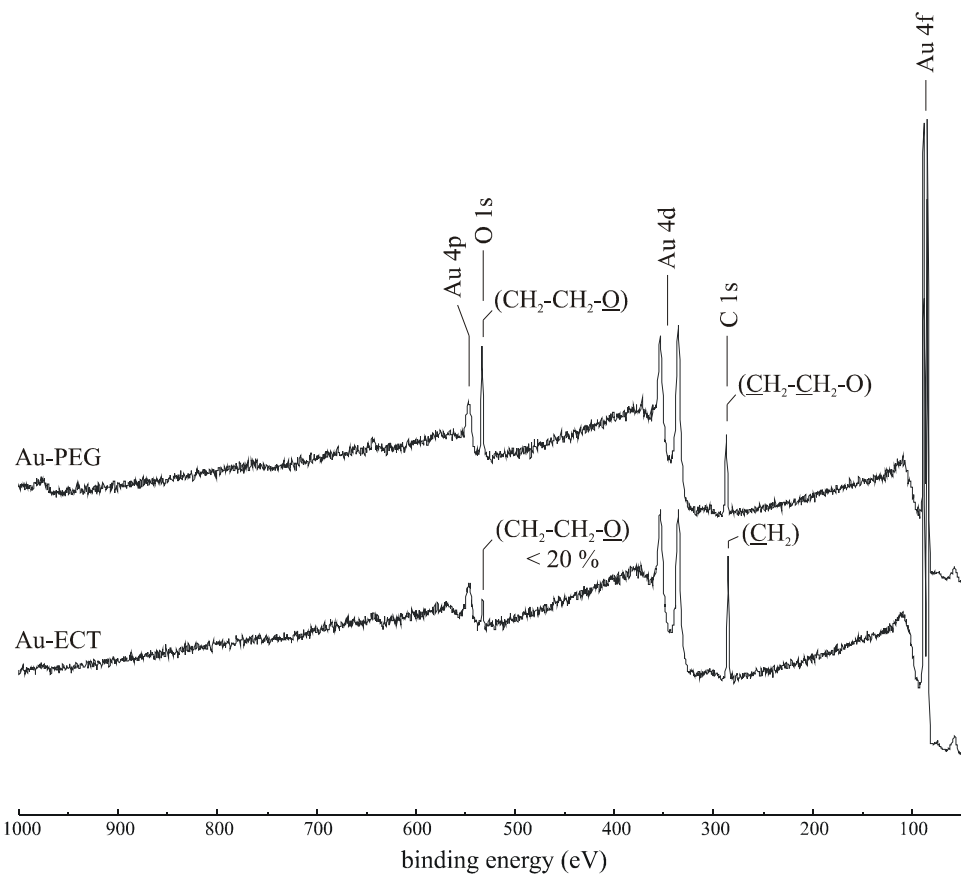


Figure 17. The XPS spectra of a PEG monolayer inside the filling pad and an ECT monolayer outside the filling pad. The PEG monolayer is of very high purity (C 1s ascribed to contaminants smaller than 3%).

The wetting pattern was revealed by addition of a small amount of water onto the derivatized surface (Figure 18). The water resides in the PEG covered hydrophilic channels and pads.

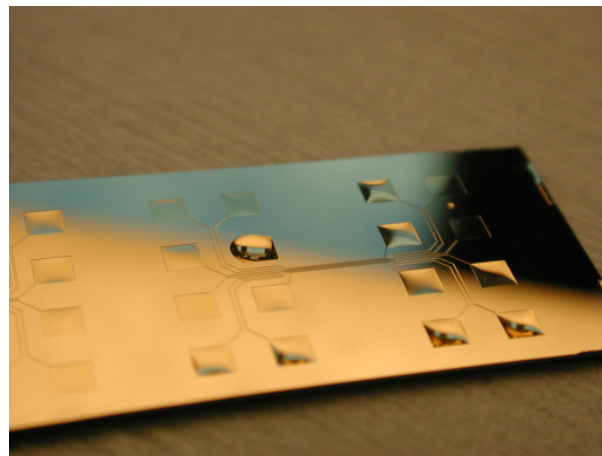


Figure 18. The wetting pattern of the thiol derivatized Au-covered wafer was revealed by addition of a drop of water. The surface inside the channels and pads, covered with PEG-thiols, has a low contact angle while the surface outside channels and pads, covered with ECT-thiols, has a high contact angle with water. The water sought contact with the surface derivatized with PEG-thiols in order to minimize its surface free energy.

The wetting behaviour of water inside channels and pads can be seen in Figure 19. Because of the small area of the pads, it was not possible to measure the surface contact angle. However, an approximation might be possible by observing and interpreting angular changes in the shape of a defined volume of liquid inside the pads (Figure 19B).

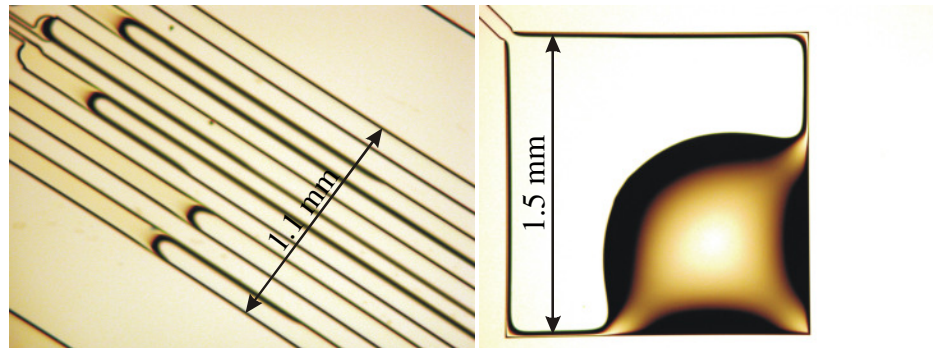


Figure 19. (A) Profiles of water advancing in the draining channels. In some channels, the water advances very far as a thin film at the intersection of the channel walls with the bottom of the channel. (B) A drop of water inside a filling pad adheres to its edges and forms a contact angle with it.

As it would be desirable to perform multiple assays with the same μ FN after a simple cleaning procedure, we tested different cleaning methods. In Figure 20 the different approaches of the methods are shown sorted by their aggressiveness towards the different surface layers.

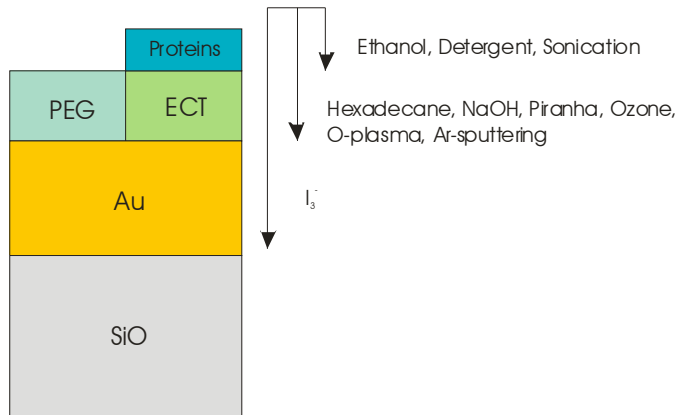


Figure 20. Different methods of cleaning the wafer surface from proteinaceous remnants vary in aggressiveness and remove more or less of the surface layers. Ethanol removes proteins and parts of the monolayers (PEG and SAM). Detergents can remove proteins but will stick to the monolayers. Sonication can reduce the reaction time. Hexadecane is a lipophile solvent and removes monolayers but not proteins from the Au surface. NaOH can tackle proteins. Piranha, Ozone and oxygen plasma are strong oxidizers and remove proteins and monolayers. Ar sputtering uses kinetic energy to mechanically clean surfaces. I_3^- can be used to remove the Au from the Si-wafer.

Most interesting would be a brief rinse with a non-aggressive solvent as for example a detergent-like SDS. Unfortunately the surface of the ECT layer is not biocompatible which means that in the current setup of the μ MIA, where blocking with BSA covers the entire region of the wafer adsorption of bovine

albumin to this area occurs. First, this is not desirable because of possible contamination of pad contents in subsequent assays performed on the same μ FN, second and more important, the physisorbed albumin has a significantly lower contact angle than ECT layers on gold, which prevents formation of a proper wetting pattern with water and thus residing of solutions inside the individual pads while filling them. Short exposure to SDS did remove proteins. Unfortunately, the PEGs are completely soluble in water and even better in Ethanol, which excludes prolonged exposure to either of them if the monolayer has not to be destroyed or at least remarkably diminished. To our knowledge there does currently not exist a satisfying method to remove proteins from ECT-SAMs on gold to receive a well defined and proper monolayer surface without damaging it or having to reform it. On the scheme in Figure 20 we therefore have to move at least one step lower towards more aggressive surface treatments for the removal of the SAMs. Established methods for removal of thiol-SAMs on gold are immersion in hexadecane for more than 20 min at 60 °C,⁷⁷ immersion in a 0.5 M solution of KOH, exposure to ozone⁷⁸ or oxygen plasma.⁷⁹ KOH is capable of disintegrating Proteins in their constituting amino acids by hydrolysis of the amino bonds, but also of dissolving Si, even at low concentrations, which is not desirable in our case. Hexadecane is not well suited to remove proteins from surfaces and investigation of the removal of proteins physisorbed to thiol-SAMs on gold do not exist to our knowledge and thorough investigation of this topic would have been necessary, which exceeds the scope of this work. A simple means to remove proteins as well as SAMs on gold is oxidation. Here, a major partition into liquid (e.g. Piranha solution) and gas phase (ozone treatment, O₂-plasma) oxidizing procedures can be made. Solvents are normally more dangerous in handling and prone to accidents than gas handling devices. O₂-plasma is a fast, simple, and widely used means to oxidize surfaces. The problem with thin gold surfaces is their destruction by the applied kinetic energy of the plasma, which will be even more accentuated at repeated exposures. Ozone is strongly oxidizing and it can be generated easily with UV radiation at two wavelengths. Chemical modification of the gold and insertion of oxygen up to a depth of a few nm into gold surfaces occurs but importantly no removal of gold from the surface. Islands of proposed double layers of alkanethiols have been observed on ozone treated gold, but not if the gold was immersed in ethanol before self-assembly for at least 10 minutes.⁸⁰ Table 2 summarizes the properties of the above-mentioned methods to clean the wafer surface in order to render it reusable.

Detergents / EtOH, Sonication	Requires much time to remove proteins with low specificity (also the thiol layer is partly removed. Detergents adsorb to Au and ECT. Poor surface definition results.)
-------------------------------	--

⁷⁷ Rogers JA, Bao Z, Makhija A, Braun P. *Adv Mater.* 1999; 11, 741.

⁷⁸ Sandhyarani N, Pradeep T. Oxidation of alkanethiol monolayers on gold cluster surfaces. *Chem Phys Letters.* 2001; 338, 33.

⁷⁹ Liao JD, Wang MC, Weng CC, Klauser R, Frey S, Zharnikov M, Grunze M. Modification of alkanethiolate self-assembled monolayers by free radical-dominant plasma. *J Phys Chem B.* Preprint, to appear 2001.

⁸⁰ Woodward JT, et al. Effect of an Oxidized Gold Substrate on Alkanethiol Self-Assembly. *Langmuir;* 2000; 16(12); 5347-5353

Piranha	Oxidizes the Au on the surface. Repeated exposure leads to delamination of Au.
Hexadecane	Does not attack the proteins. Hexadecane needs to be removed.
NaOH	Must be concentrated to effectively remove proteins and thiols, but high concentrations also dissolve the SiO wafer. We also observed delamination of Au, possibly due to preexisting microlesions in the surface.
Ozone	Temporarily modifies the Au by introduction of oxygen.
O-plasma	Changes the oxidation state of Au in an undefined manner.
Ar-sputtering	Costly instrumentation and elaborate process, although excellent surface definition. Possibly difficulties in cleaning the channel walls.
I ₃	Removes Au. Wafers need to be coated again.

Table 2. Key features of alternative methods to clean the wafers after their use in order to reuse them.

We made XPS measurements (results not shown) of the surface composition at two spots of a μ FN. The μ FN was prepared as described above, with microcontact printing (μ CP) of ECT and incubation with PEG in solution, incubated with a 1% solution of BSA for 45 min, treated with ozone under a UV lamp for 15 min, rinsed with ethanol for 3 s, and derivatized with thiols. These spectra showed no significant change in the apparition of their peaks compared to the spectra we obtained from thiol-SAMs on gold that was not treated with ozone prior to surface derivatization with thiols. We therefore conclude that cleaning with ozone as described above provides a means to clean easily the surfaces of our μ FNs from proteins and thiol-SAMs to allow reformation of thiol-SAMs without significant change in their quality.

4.4 Does Significant Depletion of Capture Antibody Occur inside Channels?

Patterned non-specific adsorption of proteins on surfaces with microfluidic networks has been studied well.^{69,17} In shallow (3 μ m) channels, depletion of proteins in the channels can be observed at low protein concentrations due to loss by adsorption.⁸¹ We tried to exclude depletion as a potential signal distortion in our experiments. We compared fluorescence intensities of patterned lines of α CRP Ab at different distances from the beginning of the channels. A solution containing α CRP antibodies at a concentration of 100 μ g mL⁻¹ was allowed to flow through the channels for 30 s before adding 500 nL of 1% BSA solution to each pad for blocking. By experience 500nL of solution require about 2 min to flow entirely through the channels. By incubating the substrate surface with drops of 50 μ g mL⁻¹ CRP and 120 μ g mL⁻¹ α CRP-FITC each in 1% BSA and for 45 min, the adsorbed stripes of α CRP could be detected with the fluorescence microscope. The area of interest was focused with 1/32 of excitation energy by insertion of neutral density filters in order to minimize photobleaching of fluorophores during this process. Focusing took about three seconds for each region. We did not measure the bleaching rate at this intensity, but it can be expected to be well under 5% of original signal, as we observed a reduction in signal of 20%

⁸¹ Caelen I, Bernard A, Juncker D, Michel B, Heinzelmann H, Delamarche E. Formation of gradients of proteins on surfaces with microfluidic networks. Langmuir. 2000; 16, 9125.

between first and second exposure, when taking two consequent frames, each during 16 s at $\frac{1}{4}$ of excitation intensity (assuming a linear behaviour of photobleaching during the 30 first seconds of illumination).

Comparison of the fluorescence signal intensity of stripes at different distances from their starting point revealed no significant change as would be expected for depletion of α CRP antibodies. We can therefore conclude that no depletion of α CRP in the channels occurs when a solution of $100 \mu\text{g mL}^{-1}$ is allowed to flow for at least 30 s through the channels. This is important to establish linear correlation between analyte concentration and fluorescence signal intensity.

4.5 Does Variation of pH Significantly Change Binding Rates?

Speed of protein adsorption, when non-specific, depends among other factors on the properties of surface (hydrophobic/ hydrophilic, surface charge) and on the total charge of the proteins. Generalization can not be made, as certain proteins, especially larger ones fibrinogen, pyruvat kinase, γ -globulins), seem to adsorb both, on hydrophilic and hydrophobic surfaces, whereas smaller proteins adsorb only to hydrophobic surfaces.⁶¹ However, protein adsorption depends also on the total charge of the proteins, which varies with ambient pH. In order to evaluate the correlation of mouse IgG1 α CRP adsorption on PDMS with pH, we made solutions of α CRP with different pH (acetate 5.0, PBS 6.0, PBS 7.0, PBS 8.0, Tris HCl 9.0). Charge of proteins and their adsorption behaviour also depend to a certain extent on the buffer used as well as its molar concentration.^{82,83} Therefore, we cannot entirely isolate the pH parameter with this experiment. The data obtained revealed no significant change of signal with variation of pH at a concentration of $100 \mu\text{g mL}^{-1}$ α CRP IgG. This conforms to the finding that such variations mainly occur at low IgG concentrations.⁸⁴ We therefore decided to use the standard PBS buffer with a pH of 7.2 and a molarity of 150 mMol L^{-1} .

4.6 Capture and Detection Antibody Concentrations

Monoclonal antibodies are an expensive good, and one does not want to use large quantities of them, when the same result can be obtained with smaller ones. Clearly, one expects simple saturation behaviour for the relation of signal intensity and concentration of detection antibody, although background might impose some troubles at very high concentrations, where BSA does not anymore dominate the dynamic equilibrium numerically. Quite differently, the variation of capture antibody concentration is more complex. Usually, proteins like to extend or flatten themselves on surfaces more or less, depending whether they tend to be rigid or flexible and on their concentration in the

⁸² Finette GM, Mao QM, Hearn MT. Comparative studies on the isothermal characteristics of proteins adsorbed under batch equilibrium conditions to ion-exchange, immobilized metal ion affinity and dye affinity matrices with different ionic strength and temperature conditions. *J Chromatogr.* 1997; 763, 71.

⁸³ Lindeberg J, Srichaiyo T, Hjerten S. High-performance adsorption chromatography of transfer ribonucleic acids and proteins on 2-microns spherical beads of hydroxyapatite. Influence of sodium chloride and magnesium ions on the resolution. *J Chromatogr.* 1990; 499, 153.

⁸⁴ Butler JE et al. The immunochemistry of sandwich ELISAs--VI. Greater than 90% of monoclonal and 75% of polyclonal anti-fluorescyl capture antibodies (CAbs) are denatured by passive adsorption. *Mol Immunol.* 1993 Sep;30(13):1165-75.

liquid phase, to e.g. present hydrophobic sections to a hydrophobic surface when in hydrophilic medium. Higher concentration in the liquid phase means denser packing on surfaces. Considering possible steric hindrance of the antigen when confronted with densely packed IgG on a surface, one could expect an optimum concentration for capture antibodies to receive maximum number of bound antigens, which has also been observed experimentally.¹⁴ Figure 21 presents the results obtained. We chose 100 $\mu\text{g mL}^{-1}$ of αCRP as working concentration for further experiments.

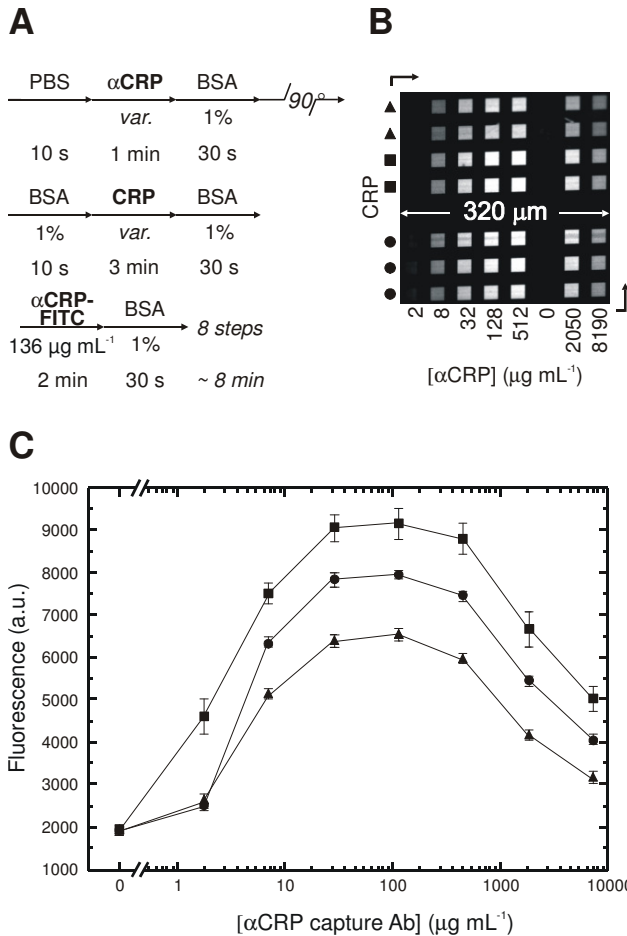


Figure 21. Influence of the concentration of αCRP Ab used to capture CRP on PDMS on the efficiency of the sandwich immunoassay. (A) The steps of the assay for CRP are denoted by arrows. The relevant reagents or buffers are indicated above the arrows; their concentration and the duration of the step are indicated below them. The bent arrow indicates the separation of the PDMS substrate from the microchannels and its repositioning onto a fresh μFN after rotation by 90°. (B) The μFN can be loaded with up to eight different solutions (1 per microchannel) before and after rotating the PDMS substrate. There is thus a maximum of 64 sites of the PDMS that can be exposed to different solutions of proteins. Captured CRP is detected with fluorescently-labeled αCRP Abs, which yields a mosaic of fluorescence. All the vertical channels except one were filled with solutions of αCRP Abs at different concentrations, and the horizontal channels were filled with CRP in PBS at 0.5 (▲), 5 (●) or 50 $\mu\text{g mL}^{-1}$ (■). (C) The mean intensities of the fluorescence signals forming the mosaic are plotted against the concentration of αCRP Ab. The lines serve as guides to the eye.

Figure 22 presents signal dependence on the concentration of detection antibodies. The background due to non-specific adsorption increased only slightly with 3400 $\mu\text{g mL}^{-1}$ of $\alpha\text{CRP-FITC}$, which can be explained with the decrease of the quotient concentration of BSA over concentration of αCRP .

FITC. As future working concentration, we chose $120 \mu\text{g mL}^{-1}$ of $\alpha\text{CRP-FITC}$. This would compensate for dilution effects due to small residues of BSA and analyte solution inside the loading pads.

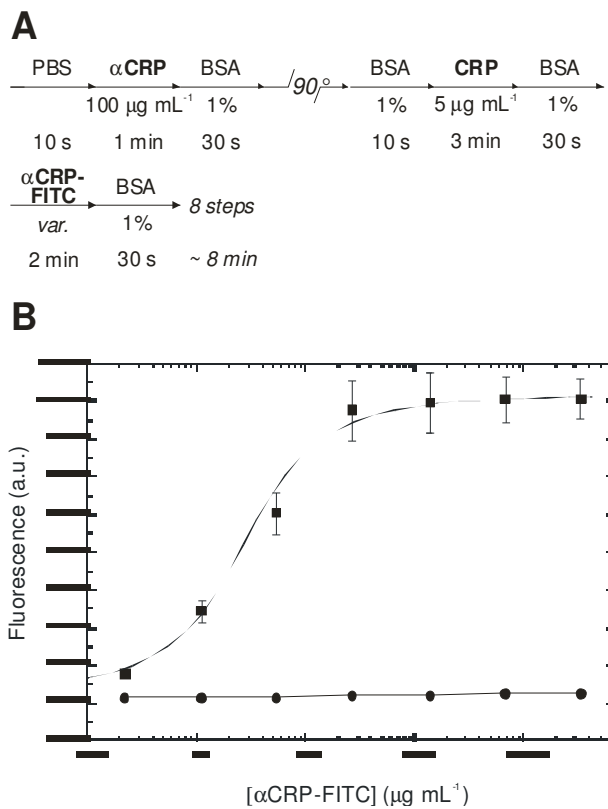


Figure 22. Optimization of the concentration of detection Ab in PBS to detect captured CRP. (A) αCRP at a concentration of $100 \mu\text{g mL}^{-1}$ in PBS was deposited onto PDMS to capture CRP from a $5 \mu\text{g mL}^{-1}$ solution in PBS. The concentration of $\alpha\text{CRP-FITC}$ detection Abs was varied. (B) The fluorescence signal varied with the concentration of detection Abs (■), whereas a background fluorescence signal (●) remained constant when no CRP was present in the solution.

4.7 Time Dependency of Analyte Binding

The binding of the analyte molecules can be expected to be time dependent due to stochastic collisions with the specific binding sites of the capture antibodies until an equilibrium state has been reached. For details, see the remarks on the Scatchard model earlier in this document. As the orientation of the analyte molecule also is important, the correct epitope has to be presented to the antibody's binding region, the time until saturation can be increased, compared to the simple, not orientation dependent physisorption on surfaces. The reasons we want to know the time course are on one hand the want for strong signals, even at low concentrations and second the urge to minimize inter-assay variances. This second argument can be understood, if one looks at the shape of the curve in Figure 23 at $t = 40$ s and at $t = 280$ s. At the former place, the curve is much steeper than in the latter, which means, that a small change dt in incubation time at $t = 40$ s produces a larger change in signal dI , than at $t = 240$ s. In order to assess the time course of CRP binding to physisorbed capture antibodies, we let a $0.1 \mu\text{g mL}^{-1}$ CRP solution in BSA

flow through the 8 channels on the same wafer for different times (40 s, 80 s, 120 s, 160 s, 200 s, 240 s and 280 s).

Introducing the association and dissociation rate constants k_1 and k_2 into equation (5) yields a kinetic representation of the binding dynamics.

$$(7) \quad \frac{d[sL]}{dt} = k_1[s][L] - k_2[sL]$$

where t is the time. The amount of bonds forming per time unit increases when the concentration $[L]$ rises. This means, that for higher concentrations of CRP, the slope of the saturation curve will be much steeper than the one for the $0.1 \mu\text{g mL}^{-1}$ CRP we chose for the experiment. When one intends to measure concentrations no smaller than $0.1 \mu\text{g mL}^{-1}$ CRP in the samples, the time necessary for the capture binding reaction will be around 180 s to reach a reasonable level of saturation (more than 80 % approximated by curve fitting of the data obtained).

The equation, which can be used to describe the saturation behaviour, can be written as

$$(8) \quad I = a(1 - e^{-bt})$$

where I is the amount of analyte bound, a the amount of analyte bound for $t = \infty$ and b a time constant which governs the slope of the curve.

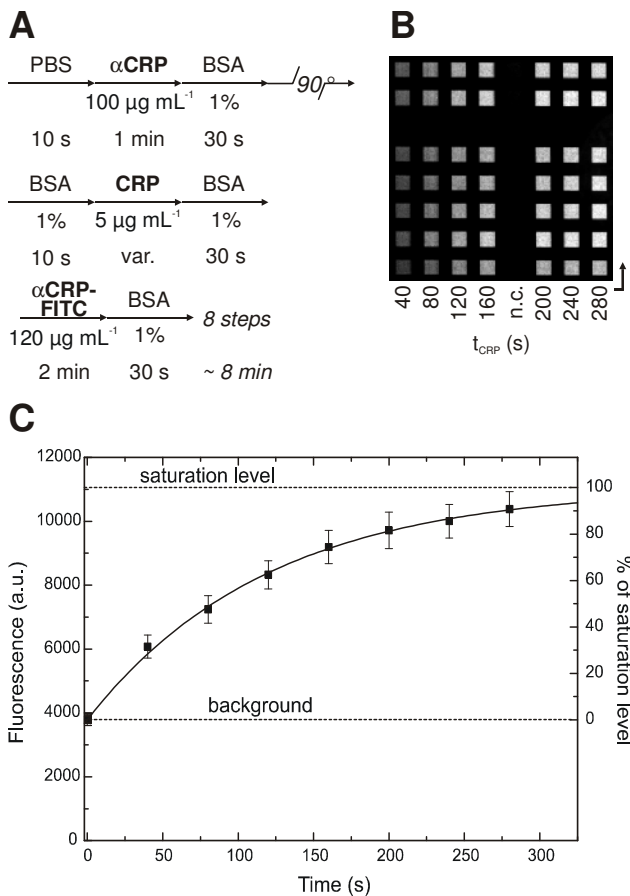


Figure 23. Effect of the time on capturing CRP on the fluorescence signal of the sandwich immunoassay. (A) The optimal concentrations of αCRP and $\alpha\text{CRP-FITC}$ in PBS were determined in the previous assays; the concentration of CRP in PBS was $0.1 \mu\text{g mL}^{-1}$. (B)

Solutions of CRP were flushed in the microchannels for variable durations (vertical lines), and the fluorescent signals corresponding to the detection of captured CRP were recorded, averaged along the vertical lines and plotted in (C) against the duration of capture. The fluorescence saturates as the duration for capture becomes sufficient to occupy a maximum of capture sites with CRP. The maximum expected signal is extrapolated from the fit. A capture step duration of 180 s is sufficient to achieve ~80% of the maximum signal for the conditions selected here.

4.8 Assay Variance and Spot Quality

The accuracy of an immunoassay depends on some major factors, such as the variability of the signals (intra- and inter-assay), the characteristics of the reference curve (i.e. binding behaviour of the Abs) and the resolution of the signal intensity. The characteristics of the reference curve can be matched to requirements by choosing appropriate Abs, while the resolution of the signal intensity is limited by the photo-registration device. Especially the variability is influenced by multiple, in part environmental, parameters (photobleaching, quality of materials, temperature, reaction time, concentrations of reactants) that are sensible. It is therefore crucial to minimize the influence of these potential noise generators. The fluorophores FITC and TRITC exhibit rapid photobleaching. The problem can be minimized with the use of novel fluorophores with improved photo-stability, such as CyTM labels. The microfluidic networks have to be inspected microscopically prior to use in order to exclude defects and contaminations. The liquids have to be filtered prior to use in order to prevent obstruction by microscopic particles (usually present in most protein dilutions). The temperature can be held at constant levels. The reaction time should neither be shortened nor extended. This is difficult when pipetting manually, but the problem could be resolved with automatic instrumentation. The manual dilution of reactants should be addressed with care.

We determined the intra-assay variability of a μMIA for CRP (Figure 25A) by taking into consideration measures limiting variability. The CRP concentration of all the eight samples was 0.1 $\mu\text{g mL}^{-1}$. The c.v. of the resulting 64 fluorescence signals was 4.4%. This is sufficient for clinical applications (< 5%). However, we still see a possible improvement and estimate the minimal c.v. of μMIAs to be less than 2%. The quality of the single spots was examined at larger magnification. The quality of shape and border (Figure 25C) as well as the overall signal uniformity, visualized with a horizontal profile plot (Figure 25D), of the spots are excellent. Improvements of the spot quality would be difficult to obtain and only minimally affect the intra-assay signal variability.

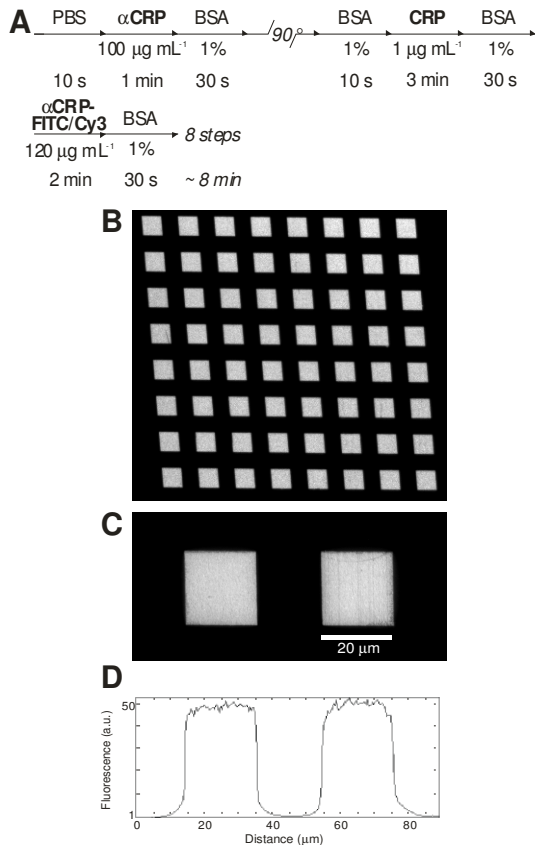


Figure 24. Quality assessment of the fluorescence signal of a μ MIA for CRP. (A) Conditions for the detection of CRP were identical for all channels and used (B) FITC-labelled or (C) Cy3-labeled α CRP detection Abs. (B) This mosaic has 64 sites with a fluorescent signal varying by only 4.4%. (C) This high-resolution fluorescence image reveals the resolution, contrast and homogeneity of two adjacent sites of a μ MIA. (D) Profile of the fluorescence intensity measured along the middle of the two sites shown in (C). These results show the high quality of the signals in the micromosaic in terms of inter- and intra-spot variations.

4.9 Reference Curve

In order to derive the concentration of the analyte from the fluorescence signal of test samples a signal-concentration function is needed. This function can be approached experimentally with the measurement of fluorescence signals of samples with known concentrations of analyte.

The solvent of reference samples should be identical with the solvent of the test samples. This can exclude inaccuracies due to interferences of the solvent with the testing method, also described as matrix effect.²⁰ In order to eliminate the physiological level of CRP in the reference samples we purified human plasma by affinity chromatography. Protein A covered sepharose was saturated with rabbit polyclonal α CRP IgG. One mL of human plasma was affinity purified. In order to demonstrate the absence of CRP in the purified plasma we compared its fluorescence signal with the background signal of a control (PBS) in a μ MIA. No significant difference between the two signals was observed, which confirmed the absence of CRP in the purified plasma. We then generated reference samples by spiking the human plasma samples with CRP in order to receive CRP concentrations ranging from 0.1 to 10 μ g mL⁻¹. The reference samples were applied in a μ MIA (Figure 25A). The

reference curve obtained has a dynamic range from 0.1 to 10 $\mu\text{g mL}^{-1}$ (Figure 25B). The concentration ranges of CRP in CHD ($0.1 - 0.5 \mu\text{g mL}^{-1}$) and SI ($10 - 100 \mu\text{g mL}^{-1}$) can be covered with the range of the assay either directly or by dilution of the test sample. It therefore seems realistic that the current configuration of αCRP antibodies might become integrated in a POC test for CRP.

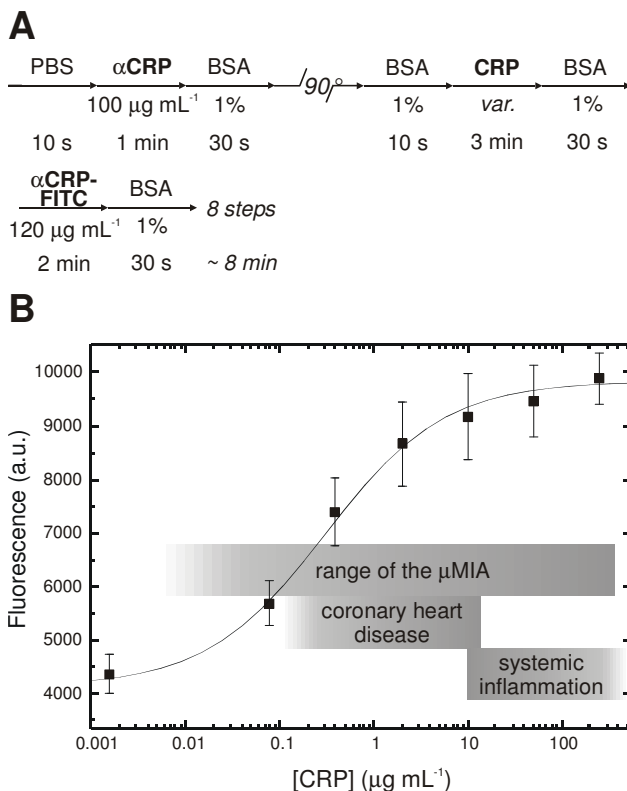


Figure 25. Reference curve for CRP-free human plasma spiked with CRP. (A) The concentration of CRP added to human plasma samples was the only parameter varied in this sandwich immunoassay. (B) The fluorescence signals obtained from the corresponding μMIA (not shown) can be fitted with a sigmoid curve. The assay is sensitive enough to cover the lower ranges of CRP of CHD and systemic inflammation conditions.

4.10 Detecting Multiple Markers in Human Plasma Simultaneously

We set up a simple demonstration of a μMIA for detecting four cardiac markers simultaneously, Figure 26. Some of the lines for capture were made redundant (Mb , $\text{S100}\alpha$ and CRP) and one line served as a negative control (PBS). The detection step was performed by filling all loading pads with the same cocktail having detection Abs against all putative markers, Figure 26A. The prerequisite for performing such combinatorial μMIA is the absence of cross reactivity between the different detection Abs and both the capture Abs and analytes. It took ~ 8 min to perform the various steps and another ~ 2 min to separate the PDMS substrate from the μFN , and to rinse and dry it. By applying capture Abs against CRP and Abs against cardiac markers to different microchannels, the simultaneous detection of different cardiac markers was achieved. Figure 26B presents the pattern of an assay for CRP, Mb , cTnI , and $\text{S100}\alpha$ using αCRP , αMb , αcTnI , and $\alpha\text{S100}\alpha$ capture Abs, respectively. The samples were solutions of plasma, obtained from healthy subjects, to which markers were added. The mosaic of fluorescence in Figure

26 shows the expected result: There are no false negative or positive signals present in the mosaic, and redundant screening yields equivalent fluorescence signals. This indicates that no cross contamination among the microchannels and no depletion of Ab or analyte occurred during the assay.

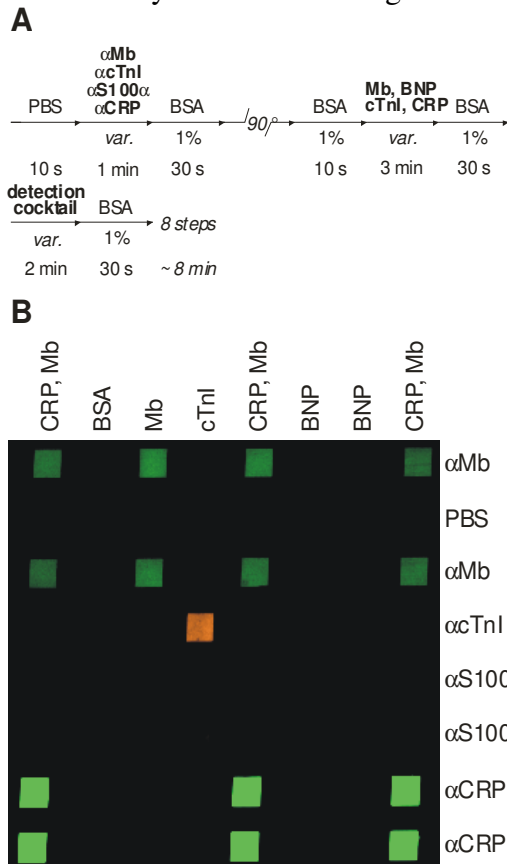


Figure 26. Simultaneous detection of cardiac markers in different samples, using a μ MIA. (A) Four capture Abs (αMb , αcTnI , $\alpha\text{S100}\alpha$, and αCRP) were deposited along horizontal lines of the μ MIA and used to detect cardiac markers that were added to plasma samples of healthy subjects. Captured markers were detected by filling microchannels (vertical direction) with a cocktail of fluorescently labelled Abs (αCRP -FITC, αBNP -Cy3, $\alpha\text{S100}\alpha$ -Cy3, αMb -FITC and αcTnI -Cy3). (B) Fluorescence microscope image, that revealing the micromosaic of binding events. As expected, no signal for $\text{S100}\alpha$ and BNP was observed due to the absence of either $\text{S100}\alpha$ in the plasma sample or αBNP capture Ab on the substrate.

5 DISCUSSION

We focused on the optimization of the μ MIA method for the quantitative detection of markers of disease in human plasma. Critical points for a potential clinical applicability of the μ MIA method are sensitivity of the assay and reproducibility of the results and therefore deserved special interest. We can divide the work in six steps as follows.

First we designed the surface properties of the μ FN wafers by covering them with gold and selectively functionalizing them with alkane thiols. The quality of the thiol monolayers inside and outside the pads of the μ FNs was verified by ellipsometry and XPS. The storage time of the functionalized wafers before their use is limited because the thiol layers on the gold surface oxidize and mix by diffusion. This issue is critical for a clinical application and methods to circumvent the problem have to be found. On top of the μ FNs we put a flow promoting sheet which allowed multiple refilling of the loading pads with different liquids. The flow of the liquids is driven only by capillary forces. A sequential filling of these ‘autonomic’ μ FNs to conduct assays has not yet been described in the literature. We see an advantage in the passive flow of liquids because no external pumping devices are necessary. The flow can still be influenced by the physical properties of the μ FNs and the flow promotion. Second, we minimized factors that could deteriorate the accuracy of the assay. Relevant depletion of α CRP capture Abs at a concentration of 0.1 mg mL^{-1} was excluded. No relevant changes in the binding behaviour of the Ab binding upon pH variations from pH 4 to pH 9 were observed. The assays were performed in a chamber of constant relative humidity ($> 85\%$). The liquids for the assay were filtered with pore sizes $< 0.22 \text{ } \mu\text{m}$ in order to exclude obstruction of the channels. Third, we evaluated the optimal values of assay parameters. With single combinatorial μ MIAs we have evaluated the optimal concentrations of capture Abs and detection Abs, respectively. The kinetics of the analyte binding reaction was analyzed in a single μ MIA in order to choose the minimal reaction time with acceptable signal intensity. We found that the total time required to perform a μ MIA is $\sim 8 \text{ min}$. Fourth, we found a low intra-assay variance (c.v. = 4.4%) and a high quality of the $20 \times 20 \text{ } \mu\text{m}^2$ spots of the assay. Measures to reduce the variance of results could include covered channels (evaporation), identical channels in the μ FNs (flow speed), automated pipetting (temporal and volumetric acuity), and the use of photostable fluorophores. Fifth, we produced a reference curve for the detection of CRP in human plasma. The dynamic range of the assay ($0.03 - 10 \text{ } \mu\text{g mL}^{-1}$) can cover the concentration ranges that are relevant for the diagnosis of CHD ($0.1 - 5 \text{ } \mu\text{g mL}^{-1}$) and SI ($> 10 \text{ } \mu\text{g mL}^{-1}$). Sixth, we performed a μ MIA with different cardiac markers in order to demonstrate the suitability of this method to detect multiple markers simultaneously.

With the μ MIA multiple markers were detected simultaneously in small volumes ($\sim 2 \text{ } \mu\text{L}$) within $\sim 8 \text{ min}$. The assay for CRP in human plasma had a sensitivity of $\sim 0.03 \text{ } \mu\text{g mL}^{-1}$ and an intra-assay c.v. of 4.4%. Common assay methods require at least $200 \text{ } \mu\text{L}$ of sample and 2 min for detection of one marker.¹⁷³ A POC test for cardiac markers requires sufficient accuracy and fast delivery of results, portability, and easy handling. The test would ideally be performed in direct vicinity to the patient in treatment with a drop of venous

¹⁷³ Sokoll, L. J.; Chan, D. W. *Anal. Chem.* 1999, 71, 356R-362R.

blood and render results that are significant for further therapeutic pathway decisions. With the use of integrated electronics/micromechanics and prepared substrates – comparable to test strips¹⁷⁴ or integrated systems¹⁷⁵ already available – these requirements could be met by the μMIA method. The μMIA can be extended to contain more than eight channels. This would allow measurement of multiple markers of disease and increase sensitivity and specificity of laboratory diagnosis.¹⁷⁶ Markers for different diseases could exclude/ diagnose diseases, while multiple markers for the same disease each add little significant information. Of course, there would remain potential problems. The selection of markers has to be done carefully with regard to possible interactions (that could be excluded with detection of potential interacting compounds) and limitations of detection (sensitivity, specificity, thermal constraints, storability). In addition, possible interference of substances present in the sample must be evaluated. The interference of haemoglobin, lipids and bilirubin with immunoassay based diagnostic tests in a dose dependent manner was reported^{177,178,179,180}. It is common practice, that manufacturers of clinical analyzers specify the allowed maximal concentration of known interfering substances to generate sufficiently accurate results.¹⁸¹ A mathematical correction algorithm for haemolysed samples was also proposed.¹⁸² Compared to clinical analyzers utilizing a solid phase immunoassay, the immunochemical reaction inside the microfluidic channels is virtually identical, the only difference being the lateral flow of the medium. In lipaemic samples, the largest particles to count with are chylomicrons (~1000nm).¹⁸³ This is much smaller than the diameter of the microchannels (20 μm). Mechanical obstruction of the channels due to microparticles in lipaemic samples therefore is unlikely. However, the interference of lipoproteins with the immunoreaction (recognition of the antigen from solution by the surface immobilized specific antibody) will presumably be the same as observed with well plate assays. However, a thorough investigation of this matter is a prerequisite prior to a clinical application of the μMIA method. An issue to be considered in fluid handling are pathologies associated with altered plasma rheological parameters, i.e. viscosity and wetting angles on the microchannel surface. The plasma viscosity varies physiologically and, more

¹⁷⁴ Fan DF. Evaluation of Beta Quik Stat kit test for pregnancy for whole blood, serum, plasma, and urine. *Clin Chem.* 1986 Feb;32(2):393.

¹⁷⁵ Apple FS et al. Simultaneous rapid measurement of whole blood myoglobin, creatine kinase MB, and cardiac troponin I by the triage cardiac panel for detection of myocardial infarction. *Clin Chem.* 1999 Feb;45(2):199-205.

¹⁷⁶ Mosca, L. *N. Engl. J. Med.* 2002, 347, 1615-1616.

¹⁷⁷ Fritz TJ, Bunker DM. Hyperlipidemia interference in radioimmunoassays. *Clin Chem.* 1982;28(11):2325-6.

¹⁷⁸ Ryder KW, et al. Effects of hemolysis, icterus, and lipemia on automated immunoassays. *Clin Chem.* 1991;37(6):1134-5.

¹⁷⁹ Glick MR, Ryder KW. Analytical systems ranked by freedom from interferences. *Clin Chem.* 1987;33(8):1453-8.

¹⁸⁰ Bossuyt X, Blanckaert N. Evaluation of interferences in rate and fixed-time nephelometric assays of specific serum proteins. *Clin Chem.* 1999;45(1):62-7.

¹⁸¹ Behring Diagnostics. Dimension CRP reagent cartridge manual. 10/98.

¹⁸² Jay DW, Provasek D. Characterization and mathematical correction of hemolysis interference in selected Hitachi-717 assays. *Clin Chem.* 1993;39(9):1804-10.

¹⁸³ Review of Medical Physiology. Ganong WF. Appleton&Lange, Stamford, 1999.

pronounced, in pathologic states – an increase of 60% and 10% was observed in patients presenting with polyarthritis and plasmocytoma, respectively.¹⁸⁴ At present, we do not know if accurate testing over the whole range of human plasma rheological parameters is feasible with one μ FN design. This point needs to be clarified prior to developing a fluidic design intended for routine clinical analyses.

The evaluation and interpretation of a vast amount of data from measured markers would require sophisticated and powerful help on software level. Multiple exceptions from rules and potential interactions would have to be considered. Emergency alerts could be included for situations that require prompt intervention. Diagnostic options and decision trees could be displayed and configured. The software would function as an interactive tool for the practising physician and require adequate instruction of the users.

At present, the μ MIA method still requires laboratory equipment and scientific knowledge. Nevertheless, applications for POC test already exist and the experience acquired by clinicians can show their advantages and disadvantages and can lead to technical and clinical process optimization. We will be able to learn from the errors of the predecessors of the μ MIA POC test. The next step towards a clinical application of μ MIA will be the comparison of measurement results obtained with the μ MIA method and with a routine hospital laboratory method. Proof of concept and further optimization of the μ MIA method will be two directions of future research that can synergise strongly.

¹⁸⁴ Blood: Rheology, Hemolysis, Gas and Surface Interactions. Ghista DN et al. (eds.), in: Advances in Cardiovascular Physics. Basel, S. Karger, 1979.

6 CONCLUSION

With the μ MIA, simultaneous detection of multiple disease markers in human plasma is possible. The μ MIA works with small sample volumes (100 μ L) and can produce results within minutes. The results of this work indicate that it should be possible to perform quantitative measurements with the μ MIA set-up used here. The μ MIA can also be extended to measure dozens of markers in dozens of samples simultaneously. This method could suit the requirements for medical applications in point-of-care testing arrangements.^{97,98} Other domains for application could include quality assurance, detection of biohazards, cellular biology, and environmental testing.

The demand for low-cost miniaturized test systems to detect biological materials (bioassays) has been increasing in the past few years. Moreover, for the near future (20 years), various economic studies forecast a substantial increase in the market volume of the bioassays segment⁹⁹. We believe that the μ MIA remains a challenging candidate in the competitive market of miniaturized bioassays. However, in order to make this imaginary scenery become reality, the readiness for substantial financial commitments and intellectual engagement is crucial.

⁹⁷ Buechler, K. F.; McPherson, P.; Anderberg, J.; Nakamura, K.; Lesefko, S.; Noar, B. in *Micro Total Analysis Systems 2001*; Ramsey, J. M. and van den Berg, A., Eds.; Kluwer Academic Publisher: The Netherlands, 2001; pp 42-44.

⁹⁸ Tüdös AJ, Besselink GA, Schasfoort RB. Trends in miniaturized total analysis systems for point-of-care testing in clinical chemistry. *Lab on a Chip*, 2001, 1(2), 83-95.

⁹⁹ Bodovitz, S.; Dunphy, J.; Gentile, F.M. The proteomics market. In: *Protein Arrays, Biochips, and Proteomics*. Marcel Dekker, 2003. Eds. Albala JS, Humphrey-Smith I.

APPENDIX A – Publications

Wolf M, Juncker D, Michel B, Hunziker P, Delamarche E. *Simultaneous detection of C-reactive protein and other cardiac markers in human plasma using micromosaic immunoassays and self-regulating microfluidic networks.* Biosens Bioelectron. **2004**, 19(10), 1193-202.

Juncker D, Schmid H, Drechsler U, Wolf H, Wolf M, Michel B, de Rooij N, Delamarche E. *Autonomous Microfluidic Capillary Systems.* Anal Chem. **2002**, 74, 6139-6144.